

Note on the $q = 2$ R -para-fermionic SYK model

Tingfei Li^{a,b}

^a*Zhejiang Institute of Modern Physics, Zhejiang University, Hangzhou, 310027, P. R. China*

^b*Kavli Institute for Theoretical Sciences (KITS), University of Chinese Academy of Sciences, Beijing 100190, China*

E-mail: tfli@zju.edu.cn

ABSTRACT: We investigate the $q = 2$ SYK model with R -para-particles (R -PSYK₂), analyzing its thermodynamics and spectral form factor (SFF) using random matrix theory. The Hamiltonian is quadratic, with coupling coefficients randomly drawn from the Gaussian Unitary Ensemble (GUE). The model exhibits self-averaging behavior and shows a striking transition in SFF dynamics: while the fermionic SYK₂ displays a ramp behavior $\mathcal{K}(t) \sim e^{C_0 t}$ with $C_0 \sim \ln N$, the R -para-particle cases exhibit $C_0 \sim \mathcal{O}(1)$. These findings offer new insights into quantum systems with exotic statistics.

KEYWORDS: SYK model, R -para-particles, Spectral Form Factor

Contents

1	Introduction	1
2	Thermodynamics	7
2.1	Constructing the Hilbert space	7
2.2	Coherent state approach	9
2.2.1	Ordinary Fermions and Bosons	11
2.2.2	R -para-fermions with $z_R = 1 + mx$	12
2.2.3	R -para-fermions with $z_R = 1 + mx + x^2$	12
2.3	Cluster function approach	13
3	SFF	14
3.1	Coherent state approach	15
3.2	Cluster function approach	18
3.2.1	R -para-fermions with $z_R(x) = 1 + mx$	20
3.2.2	R -para-fermions with $z_R(x) = 1 + mx + x^2$	21
4	Time Evolution	24
5	Conclusion	25
A	Cluster Function Approach	26
B	Coherent State Approach	28

1 Introduction

Motivation It is well known that fundamental particles are classified into two types: bosons and fermions, with their exchange statistics governed by commutation and anti-commutation relations. When we extend beyond fundamental particles in three-dimensional space, additional statistical possibilities emerge beyond these two cases. A prominent example is anyons in two-dimensional space [1–5], which play crucial roles in topological quantum computation and quantum phases of matter.

Beyond anyons, paraparticles [6–12] constitute another important generalization of ordinary exchange statistics that can be consistently defined in any spatial dimension. First studied by Green in 1953 [6], paraparticles represent a broader class of statistics that includes

both bosons and fermions as special cases. Here we mainly consider *R*-para-particles¹ which was defined by an *R*-matrix in its commutation relations [13, 14]. As demonstrated in the two papers, *R*-para-particles can emerge as quasiparticles in condensed matter systems, suggesting their potential fundamental nature. However, recent arguments [15] have challenged this view, proposing that only bosons and fermions can exist as fundamental particles.

Nevertheless, *R*-para-particles can be engineered in condensed matter systems or quantum computing platforms, making their study both meaningful and practical. Following conventional notation, we represent the creation and annihilation operators for *R*-para-particles as

$$\hat{\psi}_{i,a}^+, \hat{\psi}_{i,a}^- \quad (1.1)$$

where $i = 1, 2, \dots, N$ denotes the site index and $a = 1, 2, \dots, m$ represents the flavor index. These operators obey generalized exchange statistics described by²

$$\begin{aligned} \hat{\psi}_{l,a}^- \hat{\psi}_{j,b}^+ &= \sum_{cd} R_{bd}^{ac} \hat{\psi}_{j,c}^+ \hat{\psi}_{l,d}^- + \delta_{ab} \delta_{lj}, \\ \hat{\psi}_{l,a}^+ \hat{\psi}_{j,b}^+ &= \sum_{cd} R_{ab}^{cd} \hat{\psi}_{j,c}^+ \hat{\psi}_{l,d}^+, \\ \hat{\psi}_{l,a}^- \hat{\psi}_{j,b}^- &= \sum_{cd} R_{dc}^{ba} \hat{\psi}_{j,c}^- \hat{\psi}_{l,d}^-. \end{aligned} \quad (1.2)$$

In this formulation, each type of parastatistics is labeled by a four-index tensor R_{cd}^{ab} satisfying the constant Yang-Baxter equation (YBE) [16–18]

$$\begin{array}{c} a & b \\ \boxed{R} \\ c & d \end{array} = \delta \left| \begin{array}{c} a \\ c \end{array} \right| \delta \left| \begin{array}{c} b \\ d \end{array} \right|, \quad \begin{array}{c} a & b & c \\ \boxed{R} & & \\ & \boxed{R} & \\ d & e & f \end{array} = \begin{array}{c} a & b & c \\ & \boxed{R} & \boxed{R} \\ \boxed{R} & & \\ d & e & f \end{array}, \quad (1.3)$$

where $R_{cd}^{ab} = \begin{array}{c} a \\ \boxed{R} \\ c \end{array} \begin{array}{c} b \\ d \end{array}$, and a line segment represents a Kronecker δ function. Note that the *R*-tensor is site-independent, which represents a non-trivial constraint. For generic *R*, this makes the operators $\psi_{i,a}^\pm$ inherently non-local - a fundamental distinction between *R*-para-particles and conventional fermions/bosons. To maintain the physical interpretation of $\psi_{i,a}^\pm$ as creation and annihilation operators, we impose the additional condition

$$\sum_{a,b} R_{cd}^{ab} \left(R_{ef}^{ab} \right)^* = \delta_{ce} \delta_{df}, \quad (1.4)$$

¹Here since parafermion has already been used extensively in the literature, so we use a different name to distinguish the paraparticles with another definitions.

²From now on, we write ψ without the hat, since no confusion should arise.

so that $\psi_{i,a}^+ = (\psi_{i,a}^-)^\dagger$. We emphasize that the special cases $R_{cd}^{ab} = \pm\delta_{ad}\delta_{bc}$ recover standard bosonic (+) and fermionic (−) statistics, demonstrating that R -para-particles constitute a natural generalization of these fundamental particle types.

Recently, a model called SYK (Sachdev-Ye-Kitaev) [19–25] and its generalizations [26–35] have been widely studied. This model consists of q -body interactions of fermions with Gaussian random couplings. Its many remarkable properties make it a good toy model for studying quantum chaos [36–39], black holes [40–42], holography [23, 43–45], and quantum matter [46–49]. Here, we briefly review its basic properties.

The SYK model is solvable in the IR limit, the large q limit, and the double-scaled limit [35] for large N . In the IR limit, it acquires conformal symmetry, and the effective action can be approximated by the Schwarzian one, indicating its duality to 2D dilaton gravity. Its double-scaled limit has connections to dS holography [50–52]. Moreover, it exhibits an exponentially decaying out-of-time-ordered correlator (OTOC) with the maximal exponent $\frac{2\pi}{\beta}$ [22, 36] and a linear ramp in its SFF, serving as signatures of quantum chaos.

We are interested in the properties of the SYK model constructed with R -para-particles, which we refer to as R -PSYK for simplicity.³ Since the path integral method plays a crucial role in evaluating the SYK model, we now explore whether it still applies to R -PSYK. However, there is a key difference between ordinary particles and R -para-particles.⁴ For nontrivial R , the “creation” and “annihilation” operators of R -para-particles are global, even if they can be written as matrix product operators (MPOs) of local spin operators by a significant generalization of the Jordan-Wigner transformation (JWT) [13]. The complicated exchange statistics make it difficult to derive a path integral formulation.⁵ Although any local operator in a finite-dimensional Hilbert space can be expressed in terms of fermionic creation and annihilation operators—enabling a path integral formulation in principle, or alternatively, the use of coherent state path integrals—the Hamiltonian’s nonlocality may make the resulting expression too cumbersome for practical applications.

Beyond the path integral method, the statistics of random coupling coefficients may simplify the problem in certain limits. For example, in the double-scaled limit [35], ensemble-averaged moments $\text{tr}H^k$ can be calculated analytically, as exchanging two Hamiltonians in the trace only introduces a factor, simplifying the construction of the partition function and correlation functions. However, for R -PSYK, exchanging two operators leads to complex results, so we do not expect similar simplifications in the double-scaled limit.

As a first step, it is natural to consider the simplest case: the non-interacting para-SYK model with $q = 2$. While the SYK model is typically studied for $q > 2$ (since a simple transformation can reduce the $q = 2$ case to a free model that might appear trivial), disorder in the couplings can still produce interesting physics. Although the $q = 2$ model loses some

³There are other ways to introduce paraparticle properties in the SYK model. For example, as shown in [53], one can vary the parameter μ such that the solution to the Schwinger-Dyson equation interpolates between fermionic and bosonic behavior, with the intermediate region corresponding to a para-SYK description.

⁴Here we do not consider the trivial case where statistics returns back to fermions or bosons.

⁵A simpler alternative is to consider commuting SYK models, as explored in [54, 55].

key features of the standard SYK, the SYK₂ model retains several nontrivial characteristics. Most notably, it displays an exponential ramp in its spectral form factor (SFF), a feature numerically verified in [56] that signals chaotic behavior. Beyond the exact solvability of its Green’s function, the simplicity of SYK₂ enables a precise analysis of its level statistics. Its SFF can be understood using random matrix theory techniques [57] as well as the $G\Sigma$ path integral formalism [58–60]. Moreover, the tractability of SYK₂ allows for exact verification of eigenstate thermalization (ETH) [61] and detailed studies of eigenstate entanglement [62, 63]. Further analysis of the SFF for SYK₂ can be found in [64]. For a comprehensive review of the $q = 2$ SYK model, we refer to [65].

	R -para-fermions	Dual R -para-bosons
Ordinary	$(1+x)^m$	$(1-x)^{-m}$
Example A	$1+mx$	$(1-mx)^{-1}$
Example B	$1+mx+x^2$	$(1-mx+x^2)^{-1}$

Table 1. The single-mode partition functions of the three types of R -para-fermions and their dual R -para-bosons are studied in this paper. The function $z_R(x) = 1+mx$ is obtained when $R_{cd}^{ab} = -\delta_{ac}\delta_{bd}$, whereas $z_R(x) = 1+mx+x^2$ corresponds to $R_{cd}^{ab} = \lambda_{ab}\xi_{cd} - \delta_{ac}\delta_{bd}$. Here, the matrices λ and ξ satisfy the conditions $\lambda\xi\lambda^T\xi^T = \mathbf{1}$ and $\text{Tr}(\lambda\xi^T) = 2$.

The model In this paper, we mainly study the $q = 2$ SYK model constructed by R -para-particles, which we refer to as R -PSYK₂, with the Hamiltonian

$$H = \sum_{a=1}^m \sum_{1 \leq i, j \leq N} (h_{ij} - \mu\delta_{ij}) \psi_{i,a}^+ \psi_{j,a}^- \quad (1.5)$$

where h_{ij} is a random matrix drawn from the Gaussian unitary ensemble (GUE). Here, $i, j = 1, 2, \dots, N$ label the sites, and $a = 1, 2, \dots, m$ is the flavor index. We always impose the unitary condition in Eq. (1.4), ensuring that $\psi_{i,a}^+ = \psi_{i,a}^\dagger$ throughout the paper.

The model can be transformed into a free model via the substitution $\psi_{i,a}^- \rightarrow U_{ij} \tilde{\psi}_{j,a}^-$, where U_{ij} diagonalizes h_{ij} . The new operators satisfy the same commutation relations, so we will not distinguish them. As in ordinary fermionic/bosonic systems, we interpret $\psi_{i,a}^+$ and $\psi_{i,a}^-$ as the “creation” and “annihilation” operators of R -para-particles. We define the vacuum state by $\psi_{i,a}^- |0\rangle = 0$ for all i, a , and construct n -particle states as $\psi_{i_1, a_1}^+ \psi_{i_2, a_2}^+ \dots \psi_{i_n, a_n}^+ |0\rangle$ for a given site.

We find that the thermodynamics and SFF of the model depend **only** on the dimension of the n -particle Hilbert space (or the degeneracy of the n -th level), denoted by d_n for $n = 0, 1, 2, \dots$. The value of d_n is determined by the choice of the R -matrix. This information can

be encoded in the single-mode partition function

$$z_R(x) \equiv \sum_{n=0}^{\infty} d_n x^n \quad (1.6)$$

For ordinary fermions and bosons with m flavors, the single-mode partition functions are given by

$$z_{\text{Fermion}}(x) = (1+x)^m, \quad z_{\text{Boson}}(x) = (1-x)^{-m}. \quad (1.7)$$

In this paper, we adopt a simplified terminology: *R*-para-fermions refer to *R*-para-particles with a finite polynomial partition function $z_R(x) = \sum_{n=1}^L d_n x^n$ (where L is finite), while *R*-para-bosons describe *R*-para-particles with a fractional $z_R(x)$. Since R satisfies the Yang-Baxter equation (1.3), so does $-R$, leading to a duality between *R*-para-bosons and *R*-para-fermions:

$$z_R(x)z_{-R}(-x) = 1. \quad (1.8)$$

When $R_{cd}^{ab} \neq \pm\delta_{ad}\delta_{bc}$ but $z_R(x) = (1+x)^m$ or $(1-x)^{-m}$, we say the *R*-PSYK₂ is *trivial*, as it shares the same grand canonical partition function and SFF with the fermionic/bosonic SYK₂.⁶ In this work, we study *R*-PSYK₂ with three distinct forms of $z_R(x)$ and their duals, as summarized in Table 1. Thus, Example A ($m = 1$) and Example B ($m = 2$) correspond to trivial *R*-PSYK₂. Here, notice that the unitary condition in Eq. (1.4) cannot be satisfied for Example B with $m \geq 3$ for any λ, ξ . As a result, we never have $\psi_{i,a}^+ = (\psi_{i,a}^-)^\dagger$ in this case. However, the calculation of the partition function and SFF depends only on d_n , meaning the physical results in the paper remain valid. Nevertheless, care must be taken when computing correlation functions of ψ .⁷

Main results As discussed earlier, studying the *R*-PSYK model using the path integral method is not convenient. In this paper, we primarily analyze the model in the large N limit using random matrix theory. Our focus is on the thermodynamics and the SFF of the model. Additionally, we examine the time evolution of the model and demonstrate that computing any correlation functions is tractable. We develop a coherent state approach, detailed in Appendix B, which enables us to derive an exact expression for the averaged grand partition function and provides a simple proof of the self-averaging properties of *R*-PSYK₂. Furthermore, this coherent state approach accurately captures the early-time behavior of the SFF. The exponential ramp behavior is investigated using the cluster function method, revealing a striking difference between fermionic and (nontrivial) *R*-para-particle systems. The ramp exponent and the onset time t_p are determined by a constant C_0 . For the fermionic SYK₂ model, $C_0 \sim \ln N$, whereas for *nontrivial* *R*-PSYK₂ in Table 1, $C_0 \sim \text{const}$ in the large

⁶While these cases are not entirely trivial—they may yield distinct correlation functions compared to conventional SYK₂—here we focus primarily on their thermodynamics and SFF.

⁷We thank Zhiyuan Wang, an author of [13], for pointing this out.

N limit, leading to a transition in the SFF shape. As an example, taking $z_R(x) = 1 + mx$, we find

$$\begin{aligned}
K_{t \ll 1} &= \frac{g_0^N e^{N \frac{r_1 J_1(2t)}{t} \cos(\mu t)}}{D^{2N}} \exp \left[2N (B_1 - \rho_1) \cos(\mu t) + N (B_0 + \log(\rho_1^2 + 2\rho_1 \cos(\mu t) + 1)) \right], \\
K_{1 \ll t \ll N} &= \frac{g_0^N e^{N \frac{r_1 J_1(2t)}{t} \cos(\mu t)}}{D^{2N}} \exp [NB_0 + C_0 t], \\
K_{t \gg N} &= \frac{g_0^N e^{N \frac{r_1 J_1(2t)}{t} \cos(\mu t)}}{D^{2N}},
\end{aligned} \tag{1.9}$$

where J_1 is the Bessel function. The constants g_0 , r_1 , B_0 , and C_0 are functions of m , as defined in the main text. As discussed in [57], SYK₂ exhibits an exponential ramp. Explicitly, we have

$$K_{t_p \ll t \ll N} \sim \exp(C_0 t). \tag{1.10}$$

The transition time t_p and exponent C_0 depend on m as

$$t_p \sim \begin{cases} N^{2/5} & m > 1, \\ \left(\frac{N}{\ln N} \right)^{2/5} & m = 1, \end{cases} \quad C_0 \sim \begin{cases} \mathcal{O}(1), & m > 1, \\ \mathcal{O}(\ln N), & m = 1. \end{cases} \tag{1.11}$$

This shows a dramatic transition between the fermionic SYK₂ (or trivial R -PSYK₂ with $m = 1$) and the nontrivial fermionic R -PSYK₂ ($m > 1$). Moreover, the plateau height depends on m via

$$\frac{g_0^N}{D^{2N}} = \frac{(m^2 + 1)^N}{(m + 1)^{2N}} \geq \frac{1}{D^N} = \frac{1}{\dim(\mathcal{H})}, \tag{1.12}$$

indicating that the plateau for R -para-particles is larger than that of a regular chaotic system, as shown in Fig. 3.

Structure of the paper We study the thermodynamics in Section 2. Using the coherent state approach, we derive analytical expressions for the ensemble-averaged partition function and prove the self-averaging property of the model. We also discuss the high-temperature expansion and compare the results for different cases of R -para-particle statistics. In Section 3, we study the two-point SFF of the R -PSYK₂ model in the large N limit. Using both the coherent state approach and the cluster function method, we derive the early-time, ramp, and plateau behaviors of the SFF. We highlight a dramatic transition in the ramp behavior between ordinary fermions and R -para-fermions, characterized by the exponent C_0 . In Section 4, we discuss the time evolution of operators in the model. We outline the methodology for calculating correlation functions, including both two-point functions and OTOCs, while deferring explicit calculations to future work. In Section 5, we summarize our findings, with particular emphasis on the transition in the SFF ramp behavior. We also suggest promising

directions for future research, including studies of R -PSYK $_q$ models with $q > 2$ and more detailed investigations of correlation functions. Finally, Appendix A provides detailed derivations of the cluster function method, while Appendix B presents the coherent state approach for evaluating ensemble-averaged quantities.

2 Thermodynamics

In this section, we begin by reviewing the Hilbert space construction of the model, following the approach outlined in [13]. This construction naturally leads to a factorized expression for the partition function $Z_{\beta,\mu}$. Using the coherent state approach, we then evaluate its ensemble average and derive an analytical expression in terms of Bessel functions. We verify these results through two independent methods: high-temperature expansion and numerical simulations, finding excellent agreement between them. Furthermore, we examine a cluster approach implementation, which unfortunately fails to produce correct results. This leads us to conclude that the cluster method with a rough kernel is unsuitable for finite temperature scenarios.

2.1 Constructing the Hilbert space

A general Hamiltonian with quadratic interactions can be expressed as

$$H = \sum_{ijab} \left(h_{iajb}^{+-} \psi_{i,a}^+ \psi_{j,b}^- + h_{iajb}^{++} \psi_{i,a}^+ \psi_{j,b}^+ \right) + \text{h.c.}, \quad (2.1)$$

where h.c. denotes the Hermitian conjugate. For simplicity, we focus on the case

$$H = \sum_{a=1}^m \sum_{i,j} (h_{ij} - \mu \delta_{ij}) \psi_{i,a}^+ \psi_{j,a}^-, \quad (2.2)$$

where $h_{ij} = h_{ji}^*$ is drawn from the GUE. In the absence of disorder, this reduces to the model studied in [13]. Like the standard SYK model, it features all-to-all interactions. By applying a unitary transformation that diagonalizes h_{ij} ,

$$\psi_{i,a}^- \rightarrow U_{ij} \psi_{j,a}^-, \quad \psi_{i,a}^+ \rightarrow \psi_{j,a}^+ U_{ji}^\dagger, \quad (2.3)$$

the new operators ψ^\pm retain the same commutation relations, the Hamiltonian then simplifies to

$$H = \sum_{i=1}^N (\varepsilon_i - \mu) n_i, \quad n_i = \sum_{a=1}^m \psi_{i,a}^+ \psi_{i,a}^-, \quad (2.4)$$

where $[n_i, n_j] = 0$ for $i \neq j$. The vacuum state $|0\rangle$ is defined by

$$\psi_{i,a}^- |0\rangle = 0 \quad \forall i, a, \quad (2.5)$$

and the n -particle states at each site are given by

$$\psi_{i,a_1}^+ \psi_{i,a_2}^+ \dots \psi_{i,a_n}^+ |0\rangle. \quad (2.6)$$

The construction of the full basis for this model is discussed in detail in [13]. For completeness, we briefly review the formulation of n -particle wave functions here.

Let $\{\Psi_{a_1 a_2 \dots a_n}^\alpha\}_{\alpha=1}^{d_n}$ be a complete set of linearly independent solutions to the system of linear equations

$$\sum_{a'_j, a'_{j+1}} R_{a'_j a'_{j+1}}^{a_j a_{j+1}} \Psi_{a_1 \dots a'_j a'_{j+1} \dots a_n} = \Psi_{a_1 \dots a_j a_{j+1} \dots a_n} \quad (2.7)$$

for $j = 1, 2, \dots, n-1$. For fermionic or bosonic systems, this reduces to totally antisymmetric or symmetric wavefunctions respectively. Given the unitarity of the R -matrix, we normalize the coefficients such that

$$\sum_{a_1, \dots, a_n} \Psi_{a_1 \dots a_n}^{\beta*} \Psi_{a_1 \dots a_n}^\alpha = \delta_{\alpha\beta}. \quad (2.8)$$

These n -particle eigenfunctions can be used to construct a basis for our model. We then define the creation operator ⁸

$$\hat{\Psi}_{n,\alpha}^{(i)+} \equiv \frac{1}{\sqrt{n!}} \sum_{a_1 \dots a_n} \Psi_{a_1 \dots a_n}^\alpha \hat{\psi}_{i,a_1}^+ \dots \hat{\psi}_{i,a_n}^+. \quad (2.9)$$

The complete orthonormal basis for the state space consists of states of the form

$$|\alpha_1, \alpha_2, \dots, \alpha_N\rangle = \hat{\Psi}_{n_1, \alpha_1}^{(1)+} \hat{\Psi}_{n_2, \alpha_2}^{(2)+} \dots \hat{\Psi}_{n_N, \alpha_N}^{(N)+} |0\rangle, \quad (2.10)$$

where the quantum numbers $\{(n_i, \alpha_i)\}_{i=1}^N$ (with $1 \leq \alpha_i \leq d_{n_i}$) can be chosen independently. Then one can prove the orthonormality

$$\langle \beta_1, \beta_2, \dots, \beta_N | \alpha_1, \alpha_2, \dots, \alpha_N \rangle = \prod_{j=1}^N \delta_{n_j, n'_j} \delta_{\alpha_j, \beta_j}. \quad (2.11)$$

For $R_{cd}^{ab} = -\delta_{ac}\delta_{bd}$, solving Eq. (2.7) yields $d_0 = 1$, $d_1 = m$, and $d_{n \geq 2} = 0$. Similarly, for $R_{cd}^{ab} = \lambda_{ab}\xi_{cd} - \delta_{ac}\delta_{bd}$, we obtain $d_0 = 1$, $d_1 = m$, $d_2 = 1$, and $d_{n > 2} = 0$. These two cases serve as our primary examples throughout this work. The methodology presented here naturally extends to any fermionic R -PSYK₂ model with a generating polynomial $z_R(x) = \sum_{n=0}^L d_n x^n$ (where $d_{n > L} = 0$) and its corresponding bosonic dual.

For the basis states in Eq. (2.10), the energy is given by $E = \sum_{k=1}^N n_k(\varepsilon_k - \mu)$, leading to the partition function

$$Z_\beta = \prod_{i=1}^N \sum_{n_i=0}^L d(n_i) e^{-\beta(\varepsilon_i - \mu)n_i}. \quad (2.12)$$

⁸One can introduce **local** spin operators $\hat{\psi}_{i,a}^\pm$ that satisfy the same exchange relations as $\psi_{i,a}^\pm$, but commute between different sites. By the similar method, we construct **local** Hilbert space for each site, then one can see $\psi_{i,a}^\pm$ is a global operator represented by MPOs, which leads to a simple proof for Eq. (2.11).

Our primary interest lies in ensemble-averaged observables $\mathbb{E}(A)$, where A represents thermodynamic quantities such as energy and entropy. Importantly, these must be calculated from $\mathbb{E}(\log Z_\beta)$ rather than $\log \mathbb{E}(Z_\beta)$. For the regular SYK model, $\mathbb{E}(Z_\beta)$ can be conveniently computed using saddle-point analysis in the large- N limit through path integrals. The SYK model exhibits self-averaging behavior, satisfying $\log \mathbb{E}(Z_\beta) = \mathbb{E}(\log Z_\beta)$ for large N . The situation differs markedly for the R -PSYK₂ model: since Z_β factorizes into independent site contributions, $\mathbb{E}(\log Z_\beta)$ becomes significantly easier to compute. In this section, we employ the coherent state approach to evaluate $\mathbb{E}(Z_\beta)$. Remarkably, we prove that the R -PSYK₂ model remains exactly self-averaged even in the R -para-boson case.

2.2 Coherent state approach

As the partition function of R -PSYK₂ factorized for each mode, we can deal with it using the coherent state approach derived in Appendix B, here we have

$$\mathcal{G}(2u \cos \theta) = \sum_{n=0}^L d_n e^{-n\beta(2u \cos \theta - \mu)}. \quad (2.13)$$

Then we consider the expression for large N

$$\frac{1}{N} \log \mathbb{E}(Z_\beta) = \int_0^1 \int_0^{2\pi} \frac{udud\theta}{\pi} \log \left[\tilde{D} (1 + f_\beta(u \cos \theta)) \right] \quad (2.14)$$

where we have defined

$$\begin{aligned} \tilde{D} &= \sum_{n=0}^L d_n e^{n\beta\mu}, \quad \tilde{d}_{n,\beta\mu} \equiv \frac{d_n e^{n\beta\mu}}{\tilde{D}}, \\ f_\beta(u \cos \theta) &\equiv -1 + \sum_{n=0}^L \tilde{d}_{n,\beta\mu} e^{-2n\beta u \cos \theta} = -1 + \frac{1}{\tilde{D}} z_R \left(e^{-\beta(2u \cos \theta - \mu)} \right). \end{aligned} \quad (2.15)$$

Notice that $|f_\beta| \leq 1$, for $\cos \theta \neq 0$, so we can safely expand the log function

$$\frac{1}{N} \log \mathbb{E}(Z_\beta) = \log \tilde{D} + \int_0^1 \int_0^{2\pi} \frac{udud\theta}{\pi} \sum_{j=1}^{\infty} \frac{(-1)^{j-1}}{j} f_\beta^j. \quad (2.16)$$

Using the integral formula

$$\int_0^1 \int_0^{2\pi} \frac{udud\theta}{\pi} \exp[2ru \cos \theta] = \frac{2I_1(|2r|)}{|2r|}, \quad (2.17)$$

we can always write $\frac{1}{N} \log \mathbb{E}(Z_\beta)$ via $I_n(x)$ the modified Bessel functions of the first kind.

We then test if the order of taking ensemble average matters i.e., $\mathbb{E}(\log Z_\beta) \stackrel{?}{=} \log \mathbb{E}(Z_\beta)$. For any quantity has the form $\log Z_\beta = \sum_{i=1}^N \mathcal{G}(\varepsilon_i)$, we have

$$\mathbb{E}(\log Z_\beta) = N \int d\varepsilon \rho(\varepsilon) \mathcal{G}(\varepsilon). \quad (2.18)$$

Here

$$\mathcal{G}(\varepsilon) = \log \left[\sum_{n=0}^{\infty} d_n e^{-\beta(\varepsilon-\mu)n} \right] = \log \tilde{D} + \log [1 + f_\beta], \quad (2.19)$$

where $f_\beta(\varepsilon) \equiv -1 + \sum_{n=0}^{\infty} \tilde{d}_n e^{-n\beta\varepsilon}$. Using $\int d\varepsilon \rho(\varepsilon) e^{-r\varepsilon} = {}_0F_1(2; r^2) = \frac{2I_1(|2r|)}{|2r|}$, we exactly have

$$\mathbb{E}(\log Z_\beta) = \log \mathbb{E}(Z_\beta) \quad (2.20)$$

as expected for SYK model. The proof rely on the validity of the expansion in the log function, which always hold for finite D , all kinds of R -para-fermions. For a genera single model partition function, we have

$$\int d\varepsilon \rho(\varepsilon) \log \left(z_R \left(e^{-\beta(\varepsilon-\mu)} \right) \right) \stackrel{?}{=} \int_0^1 \int_0^{2\pi} \frac{udud\theta}{\pi} \log \left(z_R \left(e^{-\beta(2u \cos \theta - \mu)} \right) \right). \quad (2.21)$$

If both side have the same expansion series of $x = e^{-\beta(\varepsilon-\mu)}$ (or $x = e^{-\beta(2u \cos \theta - \mu)}$) at the origin $x = 0$ in the integration, we then have $\mathbb{E}(\log Z_\beta) = \log \mathbb{E}(Z_\beta)$. Notice $\varepsilon \in [-2, 2]$ $u \in [0, 1], \theta \in [0, 2\pi)$, x has the same variation region on both integrals. So we just need to evaluate the validity of the expansion of $f(x) = \log z_R(x)$ at the origin in the integration, it is obvious that we need to required $|x|$ is smaller than a convergence of radius \mathbf{R} , explicitly

$$e^{-\beta(\varepsilon-\mu)} < \mathbf{R}, \forall \varepsilon \in [-2, 2] \Rightarrow e^{\beta(\mu+2)} < \mathbf{R} \quad (2.22)$$

where \mathbf{R} can be obtained by evaluating equations

$$z_R(x) = \infty \text{ or } z_R(x) = 0 \quad (2.23)$$

which determines the singularities of integrand $\log(z_R(x))$. For R -para-fermions, $z_R(x)$ is polynomial of x with positive coefficients d_n , so that $\mathbf{R} = \infty$, the R -PSYK₂ is always self-averaged. For R -para-bosons, there are always singularities for $z_R(x)$ is a rational function, so that $\mathbf{R} = \text{finite}$, we need to impose Eq. (2.22). Take ordinary boson as example, we have $z_R(x) = (1-x)^{-m}$ so that $\mathbf{R} = 1$, so that the bosonic SYK₂ is self-averaged for $\mu < -2$. For the dual R -para-bosons of the R -para-fermion with $z_R(x) = \sum_{n=0}^L d_n x^n$, we have

$$z_{\text{ParaB}}(x) = \frac{1}{\sum_{n=0}^L (-1)^n d_n x^n}. \quad (2.24)$$

Then

$$\frac{\log \mathbb{E}(Z_{\text{ParaB};\beta})}{N} = - \int_0^1 \int_0^{2\pi} \frac{udud\theta}{\pi} \log \left(\sum_{n=0}^L (-1)^n d_n e^{-n\beta(2u \cos \theta - \mu)} \right). \quad (2.25)$$

One can use the similar method to deal with the integral. Actually, we have

$$\frac{\log \mathbb{E}(Z_{\text{ParaB};\beta})}{N} = - \frac{\log \mathbb{E}(Z_{\text{ParaF};\beta})}{N} \Big|_{e^{\beta\mu} \rightarrow -e^{\beta\mu}} \quad (2.26)$$

where $\mathbb{E}(Z_{\text{ParaF};\beta})$ is the partition function of dual R -para-fermionic SYK₂ with $z_R(x) = \sum_{n=0}^L d_n x^n$. Since we only consider the self-averaged theory, we just denote the averaged partition function $\mathcal{Z}_{\beta,\mu} = \mathbb{E}(Z_\beta)$, then we can calculate all other thermodynamic functions. We will test the validity of the coherent state approach displayed here by calculate the three R -para-fermionic examples listed in Table 1 and compare their high-temperature expansion with the numerical simulation results.

2.2.1 Ordinary Fermions and Bosons

As a warm up, we first consider ordinary fermions with m flavors. Since $z_R = (1+x)^m$, we have

$$\frac{\log \mathcal{Z}_F}{N} = m \int_0^1 \int_0^{2\pi} \frac{udud\theta}{\pi} \log \left(1 + e^{-\beta(2u \cos \theta - \mu)} \right) = m \sum_{j=1}^{\infty} \frac{(-)^{j-1} e^{j\beta\mu} 2I_1(2j\beta)}{j 2j\beta}. \quad (2.27)$$

Then we consider the high-temperature expansion (where we do not expand $e^{j\beta\mu}$)

$$\frac{\log \mathcal{Z}_F}{mN} = \log(e^{\beta\mu} + 1) + \frac{\beta^2 e^{\beta\mu}}{2(e^{\beta\mu} + 1)^2} + \frac{\beta^4 e^{\beta\mu} (-4e^{\beta\mu} + e^{2\beta\mu} + 1)}{12(e^{\beta\mu} + 1)^4} + \mathcal{O}(\beta^5). \quad (2.28)$$

Then we deal with ordinary bosons. For $z_R(x) = (1-x)^{-m}$, we have

$$\frac{\log \mathcal{Z}_B}{N} = -m \int_0^1 \int_0^{2\pi} \frac{udud\theta}{\pi} \log \left(1 - e^{-\beta(2u \cos \theta - \mu)} \right) = m \sum_{j=1}^{\infty} \frac{e^{j\beta\mu} 2I_1(2j\beta)}{j 2j\beta} \quad (2.29)$$

where we must impose $\mu < 0$ to make the summation convergent. As discussed before, one can obtain partition function for ordinary bosons by simply replacing $e^{\beta\mu} \rightarrow -e^{\beta\mu}$, one can check it by simply comparing Eq. (2.29) with Eq. (2.27). Its high-temperature expansion is

$$\frac{1}{mN} \log \mathcal{Z}_B = -\log(1 - e^{\beta\mu}) + \frac{\beta^2 e^{\beta\mu}}{2(e^{\beta\mu} - 1)^2} + \frac{\beta^4 e^{\beta\mu} (4e^{\beta\mu} + e^{2\beta\mu} + 1)}{12(e^{\beta\mu} - 1)^4} + \mathcal{O}(\beta^5). \quad (2.30)$$

Although the formula make sense for any $\mu < 0$, but it is derived by the expanding the log function in the integrand in Eq. (2.29), which is only valid for $\mu < -2$. Notice that -2 is the lower bound of semi-circle density $\rho(\varepsilon)$ for large N limit. For large but finite N , we may have few energy levels $\varepsilon_i < \mu$. So for numerical simulation, we regularize the definition partition function of bosonic SYK₂

$$\mathbb{E}_{reg}(Z_\beta) = \text{Real} \left(\prod_{i=1}^N \left(\frac{1}{1 + \delta \sqrt{-1} - e^{-\beta(\varepsilon_i - \mu)}} \right)^m \right) \quad (2.31)$$

where $\delta \ll 1$ is a small number choice to make keep the numerical simulation stable.

2.2.2 R -para-fermions with $z_R = 1 + mx$

For Example A with $z_R = 1 + mx$, using Eq. (2.15), we have

$$f_\beta(u \cos \theta) = -1 + \tilde{d}_0 + \tilde{d}_1 e^{-2\beta u \cos \theta}. \quad (2.32)$$

Here $d_0 = 1, d_1 = m$, it is easy to obtain the explicit expression of \tilde{d}_0, \tilde{d}_1 , we just keep the form. It is direct to obtain

$$\begin{aligned} \frac{\log \mathcal{Z}}{N} &= \log \tilde{D} + \sum_{j=1}^{\infty} \sum_{k=0}^j \frac{(-)^{j-1}}{j} \binom{j}{k} (\tilde{d}_1)^k (\tilde{d}_0 - 1)^{j-k} \frac{2I_1(2k\beta)}{2k\beta} \\ &= \log \tilde{D} + \log \tilde{d}_0 + \sum_{k=1}^{\infty} \frac{(-1)^{k+1}}{k} \left(\frac{\tilde{d}_1}{\tilde{d}_0} \right)^k \frac{2I_1(2k\beta)}{2k\beta} \end{aligned} \quad (2.33)$$

where we use the trick to exchange the summation for j and k : $\sum_{j=1}^{\infty} \sum_{k=0}^j \rightarrow \sum_{k=0}^{\infty} \sum_{j=k, j>0}^{\infty}$. To test the validity of the formula, we consider its high temperature expansion

$$\frac{\log \mathcal{Z}}{N} = \log \tilde{D} + \log \tilde{d}_0 + \log(r+1) + \frac{\beta^2 r}{2(r+1)^2} + \frac{\beta^4 r(r^2 - 4r + 1)}{12(r+1)^4} + \mathcal{O}(\beta^6). \quad (2.34)$$

Here we have defined $r = \frac{\tilde{d}_1}{\tilde{d}_0}$ for simplicity.

2.2.3 R -para-fermions with $z_R = 1 + mx + x^2$

For Example B with $z_R = 1 + mx + x^2$, using Eq. (2.15), we have

$$f_\beta(u \cos \theta) = -1 + \tilde{d}_0 + \tilde{d}_1 e^{-2\beta u \cos \theta} + \tilde{d}_2 e^{-4\beta u \cos \theta}. \quad (2.35)$$

Here $d_0 = 1, d_1 = m, d_2 = 1$, it is easy to obtain the explicit expression of $\tilde{d}_0, \tilde{d}_1, \tilde{d}_2$, we just keep the form, so that the result can easily apply to any R -PSYK₂ with $z_R(x) = d_0 + d_1 x + d_2 x^2$. Direct calculation leads to

$$\frac{\log \mathcal{Z}}{N} = \log \tilde{D} + \sum_{j=1}^{\infty} \sum_{k=0}^j \sum_{l=0}^k \frac{(-)^{j-1}}{j} \binom{j}{k} \binom{k}{l} (\tilde{d}_0 - 1)^{j-k} (\tilde{d}_2)^l (\tilde{d}_1)^{k-l} \frac{2I_1(2(k+l)\beta)}{2(k+l)\beta}. \quad (2.36)$$

The high-temperature expansion gives

$$\begin{aligned} \frac{\log \mathcal{Z}}{N} &= \log \tilde{D} + \log(\tilde{d}_0 + \tilde{d}_1 + \tilde{d}_2) + \frac{\beta^2 (\tilde{d}_1 \tilde{d}_2 + \tilde{d}_0 (\tilde{d}_1 + 4\tilde{d}_2))}{2(\tilde{d}_0 + \tilde{d}_1 + \tilde{d}_2)^2} \\ &\quad + \frac{\beta^4}{12(\tilde{d}_0 + \tilde{d}_1 + \tilde{d}_2)^4} \left[(\tilde{d}_1 + 16\tilde{d}_2) \tilde{d}_0^3 - (4\tilde{d}_1^2 + 13\tilde{d}_2 \tilde{d}_1 + 64\tilde{d}_2^2) \tilde{d}_0^2 \right. \\ &\quad \left. + (\tilde{d}_1^3 + 8\tilde{d}_2 \tilde{d}_1^2 - 13\tilde{d}_2^2 \tilde{d}_1 + 16\tilde{d}_2^3) \tilde{d}_0 + \tilde{d}_1 \tilde{d}_2 (\tilde{d}_1^2 - 4\tilde{d}_2 \tilde{d}_1 + \tilde{d}_2^2) \right] + \mathcal{O}(\beta^5). \end{aligned} \quad (2.37)$$

2.3 Cluster function approach

Cluster function approach is used to calculate the ensemble averaged SFF in [57]. As derived in Appendix A, we expected the cluster function approach still work for high-temperature case. For simplicity, we denote

$$\sum_{\{k\}}' \equiv \sum_{\{k\}, k_i=1}^L, \quad |\{k\}| \equiv \sum_{i=1}^n k_i. \quad (2.38)$$

Finally we have

$$\mathbb{E}(Z_\beta) = \exp \left[N \sum_{n=1}^{\infty} \frac{(-1)^{n-1}}{n} \sum_{\{k\}}' d_{\{k\}} e^{\sum_{i=1}^n \beta k_i \mu} I_n^E(\beta \{k\}) \right]. \quad (2.39)$$

With the explicit expressions of $I_n^E(\beta \{k\})$, we have

$$\frac{\log \mathbb{E}(Z_\beta)}{N} = \sum_k' d_k e^{\beta k \mu} {}_0F_1(2; k^2 \beta^2) + \sum_{n=2}^{\infty} \frac{(-1)^{n-1}}{n} \sum_{\{k\}}' d_{\{k\}} e^{\sum_{i=1}^n \beta k_i \mu} \frac{\sinh\left(\frac{\pi\beta}{2} \sum_{i=1}^n k_i\right)}{\frac{\pi\beta}{2} \sum_{i=1}^n k_i}, \quad (2.40)$$

where ${}_0F_1(x)$ is the confluent hypergeometric function. We replace the summation $\sum_{n=2}^N$ with $\sum_{n=2}^{\infty}$ to obtain the correct result for $\beta = 0$. This leads to alternating series that are not absolutely convergent. For example, when $z_R(x) = 1 + mx$ and $\mu = 0$, we have

$$\frac{\log \mathbb{E}(Z_{\beta=0})}{N} = m + \sum_{n=2}^{\infty} \frac{(-1)^{n-1}}{n} m^n \rightarrow \log(1 + m). \quad (2.41)$$

Therefore, one must interpret the summation in the definition of $\log Z_\beta$ as a formal expansion of $\log(1 + m)$, which is strictly invalid for $m \geq 1$. To evaluate Eq. (2.40), we recommend first performing the high-temperature expansion and then computing the summation. The high-temperature expansion can be derived by expanding for $\beta \ll 1$

$${}_0F_1(2; \zeta^2) = 1 + \frac{\zeta^2}{2} + \mathcal{O}(\zeta^4), \quad \frac{\sinh(x)}{x} = 1 + \frac{x^2}{6} + \mathcal{O}(x^4). \quad (2.42)$$

For example, for the case $z_R(x) = 1 + mx$, and $\mu = 0$, we have

$$\frac{\log \mathcal{Z}_{\beta \ll 1}}{N} = \log(m + 1) + \frac{m}{24} \left(12 - \frac{\pi^2 m(m+2)}{(m+1)^2} \right) \beta^2 + \mathcal{O}(\beta^4), \quad (2.43)$$

while the coherent state approach gives

$$\frac{\log \mathcal{Z}_{\beta \ll 1}}{N} = \log(m + 1) + \frac{\beta^2 m}{2(m+1)^2} + \mathcal{O}(\beta^4). \quad (2.44)$$

Since numerical simulations have confirmed the validity of the coherent state approach (as demonstrated in Fig. 1), we observe that the cluster function obtained from the rough kernel method is unreliable. Instead, one could consider using the refined kernel

$$\tilde{K}(\varepsilon_i, \varepsilon_j) = \frac{\sin\left(N\pi(\varepsilon_i - \varepsilon_j)\rho\left(\frac{\varepsilon_i + \varepsilon_j}{2}\right)\right)}{\pi(\varepsilon_i - \varepsilon_j)}, \quad (2.45)$$

though this would complicate analytical evaluation. Given that the coherent state approach has yielded satisfactory results, we will not pursue the refined kernel method further.

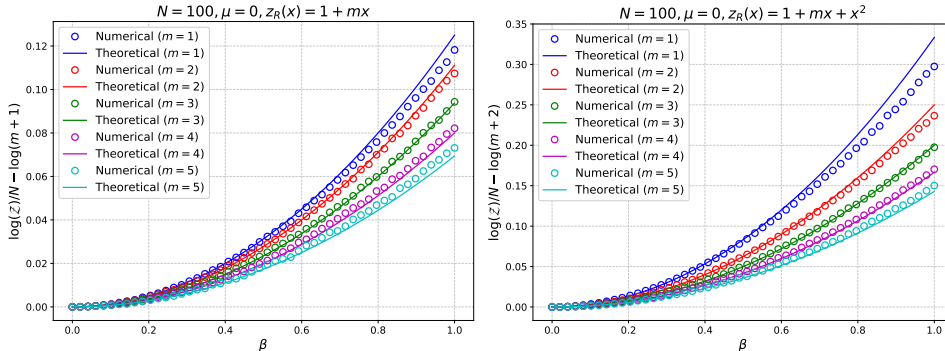


Figure 1. The plot compares the ensemble-averaged partition function for numerical simulations and theoretical expectations in two cases. For $z_R(x) = 1 + mx$, the theoretical expectation is $\log \mathcal{Z}/N = \log(1 + m) + \frac{m}{2(1+m)^2}\beta^2 + \mathcal{O}(\beta^4)$. For $z_R(x) = 1 + mx + x^2$, it becomes $\log \mathcal{Z}/N = \log(1 + m) + \frac{1}{2+m}\beta^2 + \mathcal{O}(\beta^4)$. The numerical results are averaged over 200 samples.

3 SFF

In this section, we evaluate the two-point SFF for the fermionic R -PSYK₂ model in the large N limit. The SFF is defined as

$$K(t) = \frac{1}{D^{2N}} \prod_{i=1}^N \left| \sum_{n_i=0}^L d(n_i) e^{it(\varepsilon_i - \mu)n_i} \right|^2, \quad (3.1)$$

where the prefactor $\frac{1}{D^{2N}}$ ensures the normalization condition $K(0) = 1$. We are particularly interested in its disorder-averaged value:

$$\mathcal{K}(t) \equiv \mathbb{E}[K(t)]. \quad (3.2)$$

As mentioned in the introduction, the SFF serves as a diagnostic tool for quantum chaos. Universally, it exhibits a rapid decay at early times ($t \ll 1$) and saturates to a plateau at late times ($t \gg N$). For chaotic quantum systems, the SFF typically displays a linear ramp $\mathcal{K}(t) \sim t$ in the intermediate region $t_p \ll t \ll N$. However, as shown in [57, 58], the

SYK₂ model exhibits an exponential ramp $\mathcal{K}(t) \sim \exp(C_0 t)$. The onset time scale t_p and the exponent C_0 of this exponential ramp can be determined analytically.

For the R -PSYK₂ model, we employ methods from random matrix theory to compute the SFF. In addition to the cluster function approach presented in [57], we develop a coherent state approach (detailed in Appendix B) that is particularly effective for times $t \sim \mathcal{O}(1)$ in the large N limit. Numerical results confirm that the coherent state approach accurately captures the early-time behavior ($t \sim \mathcal{O}(1)$), whereas the cluster function approach loses precision in this region due to the roughness of the box approximation.

For the intermediate time region, we rely on the cluster function approach and provide a general analysis for R -PSYK₂ with arbitrary polynomial weight functions $z_R(x) = \sum_{k=0}^L d_k x^k$. Our findings reveal a striking difference in ramp behavior: for $z_R(x) = 1 + mx$ ($m \neq 1$) and $z_R(x) = 1 + mx + x^2$ ($m \neq 2$), the exponent C_0 approaches a constant, whereas for the conventional SYK₂ model ($z_R(x) = 1 + x$ or $z_R(x) = (1 + x)^2$), C_0 scales as $\log N$. This leads to a dramatic change in the ramp behavior.

3.1 Coherent state approach

Before proceeding with calculations, we establish some key notations. We define

$$|z_R|^2(t) \equiv \left| \sum_{n=0}^L d(n) e^{it(\varepsilon - \mu)n} \right|^2 \equiv \sum_{k=0}^L g_k \cos(kt(\varepsilon - \mu)), \quad (3.3)$$

with normalized coefficients $\tilde{g}_k = g_k/D^2$ satisfying $\sum_{k=0}^L \tilde{g}_k = 1$. The ensemble-averaged SFF

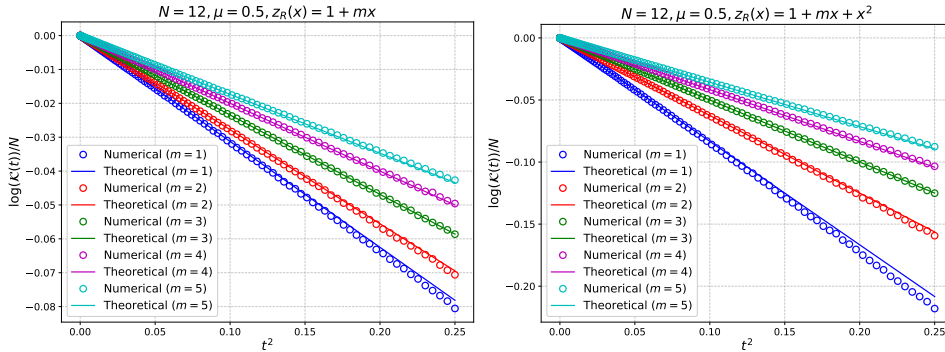


Figure 2. Short-time SFF comparison between numerical simulations (averaged over 2000 samples) and theoretical predictions from the coherent state approach, for $z_R(x) = 1 + mx$ (left) and $z_R(x) = 1 + mx + x^2$ (right).

can be evaluated using the techniques developed in Appendix B. However, two approximations limit the validity of this approach: (1) changing the order of taking the cut-off and determinant in Eq. (B.4), and (2) replacing the cut-off trace tr_N with the coherent state basis trace tr_R in Eq. (B.8). Consequently, this method is only reliable for $t \sim \mathcal{O}(1)$ in the large N limit and cannot capture the ramp behavior of R -PSYK₂.

While terms proportional to $1/R = 1/\sqrt{N}$ could be neglected, we choose to retain them. Applying the Baker-Campbell-Hausdorff formula

$$e^X e^Y = e^Z, \quad Z = X + Y + \frac{1}{2}[X, Y] + \dots, \quad (3.4)$$

we derive the coherent state representation

$$e^{a+a^\dagger} = e^{a^\dagger} e^a e^{1/2} = e^{\alpha+\alpha^*-1/2}, \quad (3.5)$$

where we have used the substitutions $a^\dagger \rightarrow \alpha^* - \partial_\alpha$ and $a \rightarrow \alpha$ in the coherent basis. As derived in Appendix B, we make the replacement $\varepsilon \rightarrow 2u \cos \theta - \frac{1}{2R}$ in Eq. (3.3), yielding

$$\mathcal{G}(2u \cos \theta) = \sum_{k=0}^L g_k \cos(kt(2u \cos \theta - \mu_R)), \quad (3.6)$$

where we have defined the shifted chemical potential $\mu_R \equiv \mu + \frac{1}{2R} = \mu + \frac{1}{2\sqrt{N}}$. The ensemble-averaged SFF then takes the form

$$\frac{\log \mathcal{K}(t)}{N} = -2 \log D + \int_0^1 \int_0^{2\pi} \frac{u du d\theta}{\pi} \log \left[\sum_{k=0}^L g_k \cos(kt(2u \cos \theta - \frac{1}{2R} - \mu)) \right]. \quad (3.7)$$

In the formal large- t limit ($t \rightarrow \infty$), where we can ignore oscillatory terms, this simplifies to the plateau value

$$\frac{\log \mathcal{K}_{t=\infty}}{N} = -2 \log D + \log g_0, \quad (3.8)$$

which correctly reproduces the expected plateau behavior. For $t \ll 1$, we have the expansion

$$\begin{aligned} \frac{\log \mathcal{K}(t)}{N} &= \int_0^1 \int_0^{2\pi} \frac{u du d\theta}{\pi} \log \left[1 - \frac{1}{2} \sum_{k=0}^L \tilde{g}_k k^2 t^2 (2u \cos \theta - \mu_R)^2 \right] + \mathcal{O}(t^4) \\ &= -\frac{1}{2} \sum_{k=0}^L \tilde{g}_k k^2 t^2 \int_0^1 \int_0^{2\pi} \frac{u du d\theta}{\pi} (2u \cos \theta - \mu_R)^2 + \mathcal{O}(t^4) \\ &= -\frac{1 + \mu_R^2}{2} \sum_{k=0}^L \tilde{g}_k k^2 t^2 + \mathcal{O}(t^4). \end{aligned} \quad (3.9)$$

Numerical verification of these results is shown in Fig. 2. For the time scale $t \sim \mathcal{O}(1)$, we have

$$\frac{\log \mathcal{K}(t)}{N} = \int_0^1 \int_0^{2\pi} \frac{u du d\theta}{\pi} \log \left[\sum_{k=0}^L \tilde{g}_k \cos(kt(2u \cos \theta - \mu_R)) \right]. \quad (3.10)$$

To facilitate analysis, we rewrite this expression as:

$$\begin{aligned} \frac{\log \mathcal{K}(t)}{N} &= \int_0^1 \int_0^{2\pi} \frac{u du d\theta}{\pi} \log [1 + F(u \cos \theta)] \\ &= \sum_{j=1}^{\infty} \int_0^1 \int_0^{2\pi} \frac{u du d\theta}{\pi} \frac{(-1)^{j-1} (F(u \cos \theta))^j}{j}, \end{aligned} \quad (3.11)$$

where we define

$$F(u \cos \theta) = -1 + \sum_{k=0}^L \tilde{g}_k \cos(kt(2u \cos \theta - \mu_R)), \quad |F(u \cos \theta)| \leq 1. \quad (3.12)$$

Using the integral identity:

$$\int_0^1 \int_0^{2\pi} \frac{u \, du \, d\theta}{\pi} \cos(kt(2u \cos \theta - \mu_R)) = \frac{J_1(2kt) \cos(k\mu_R t)}{kt}, \quad (3.13)$$

we can express $\frac{\log \mathcal{K}(t)}{N}$ as an expansion in terms of Bessel functions. For the case $z_R(x) = 1 + mx$, we obtain

$$\frac{\log \mathcal{K}(t)}{N} = \sum_{j=1}^{\infty} \sum_{k=0}^j \frac{(-1)^{j-1}}{j} \frac{r_1^j}{2^j} \binom{j}{k} \cos[(j-2k)\mu_R t] \frac{2J_1(2|j-2k|t)}{2|j-2k|t}, \quad (3.14)$$

where $r_1 = \frac{2m}{m^2+1} \leq 1$. The formula in Eq. (3.11) cannot produce the exponential ramp $\log \mathcal{K}(t) \sim C_0 t$ in the region $1 \ll t \ll N$, since it ultimately depends on terms of the form $\frac{J_1(2kt) \cos(k\mu_R t)}{kt}$. These terms have the asymptotic behavior:

$$\left| \frac{J_1(2kt)}{kt} \right| \sim \frac{1}{t^{3/2}} \ll 1 \quad \text{for } 1 \ll t \ll N, \quad k \neq 0. \quad (3.15)$$

Consequently, the SFF obtained via the coherent state approach rapidly approaches the plateau in this time region. This conclusion remains valid even when considering higher-order approximations of tr_N , as the ramp structure may be lost in the approximation of Eq. (B.4). As a concrete example, consider the first-order correction (refer to Eq. (B.17)):

$$\frac{(\log \mathcal{K}(t))^{(1)}}{N} = \int_{u_a}^{u_b} \int_0^{2\pi} \tilde{w}_1(u) \frac{u \, du \, d\theta}{\pi} \log[1 + F(u \cos \theta)], \quad (3.16)$$

with integration bounds $u_a = r_a/\sqrt{N} = 1 - v_a/\sqrt{N}$ and $u_b = r_b/\sqrt{N} = 1 + v_b/\sqrt{N}$. The weight functions are

$$\begin{aligned} \tilde{w}_1(u_a < u < 1) &= \frac{\Gamma(N, N)}{\Gamma(N)} - \frac{2e^{-N} N^{N+\frac{1}{2}} (u\sqrt{N} - \sqrt{N})}{\Gamma(N+1)} - 1, \\ \tilde{w}_1(1 < u < u_b) &= \frac{\Gamma(N, N)}{\Gamma(N)} - \frac{2e^{-N} N^{N+\frac{1}{2}} (u\sqrt{N} - \sqrt{N})}{\Gamma(N+1)}. \end{aligned} \quad (3.17)$$

Using the integral identities

$$\begin{aligned} \int u \, du \int_0^{2\pi} \frac{d\theta}{\pi} \cos(kt(2u \cos \theta - \mu_N)) &= u^2 \cos(\mu_N kt) {}_0F_1(; 2; -k^2 t^2 u^2), \\ \int u \, du \int_0^{2\pi} \frac{d\theta}{\pi} \cos(kt(2u \cos \theta - \mu_N)) &= \frac{1}{3} u^3 \cos(\mu_N kt) {}_1F_2\left(\frac{3}{2}; 1, \frac{5}{2}; -k^2 t^2 u^2\right), \end{aligned} \quad (3.18)$$

we can express $\frac{(\log \mathcal{K}(t))^{(1)}}{N}$ in terms of hypergeometric functions ${}_0F_1(; 2; -a^2 t^2)$ and ${}_1F_2\left(\frac{3}{2}; 1, \frac{5}{2}; -b^2 t^2\right)$. Both these functions (and their derivatives) exhibit oscillatory behavior with decaying amplitude, rapidly approaching zero for $t \gg 1$. Similarly, one can show that higher order corrections still do not contribute to the ramp behavior in the region $1 \ll t \ll N$.

3.2 Cluster function approach

The SFF can also be analyzed using the cluster function approach. We begin by defining

$$|z_R|^2(t) = g_0 \left(1 + \sum_{k=1}^L r_k \cos(kt(\varepsilon - \mu)) \right) \equiv g_0 (1 + F(\varepsilon - \mu, t)), \quad (3.19)$$

where $r_k = g_k/g_0$ are the normalized coefficients. An important identity emerges when considering products of F

$$\prod_{j=1}^n F(\varepsilon_j, t) = 2^{-n} \sum_{\substack{\zeta_j = -L \\ \zeta_j \neq 0}}^L \left(\prod_{j=1}^n r_{|\zeta_j|} \right) e^{it \sum_{j=1}^n (\varepsilon_j - \mu) \zeta_j}. \quad (3.20)$$

Following the methodology outlined in Appendix A, we derive the SFF expression

$$\mathcal{K}(t) = \frac{g_0^N}{D^{2N}} \exp \left[N \sum_{k=1}^L r_k \frac{J_1(2kt)}{kt} \cos(k\mu t) + N A_0(t) + 2N \sum_{p=1}^{NL} A_p(t) \frac{\sin\left(\frac{\pi}{2} p t\right)}{\frac{\pi}{2} p t} \cos(p\mu t) \right], \quad (3.21)$$

where the coefficients $A_p(t)$ are given by

$$A_p(t) = \sum_{n=2}^N (-1)^{n-1} \frac{1}{n 2^n} \sum_{\sum \zeta_i = p} r(\{\zeta_i\}) \left[1 - \frac{t}{2N} s(\{\zeta_i\}) \right] \Theta \left[1 - \frac{t}{2N} s(\{\zeta_i\}) \right]. \quad (3.22)$$

Here $r(\{\zeta_i\}) \equiv \prod_{j=1}^n r_{|\zeta_j|}$, the $s(\{\zeta_i\})$ is defined as

$$s(\{\zeta_i\}) = \max \left\{ 0, \sum_{i=1}^j \zeta_i \right\}_{j=1}^{n-1} - \min \left\{ 0, \sum_{i=1}^j \zeta_i \right\}_{j=1}^{n-1}. \quad (3.23)$$

We now analyze the SFF behavior in three distinct time regions:

- Short-to-Intermediate Times: $0 < t \ll N$

For this region, we approximate $\Theta \left[1 - \frac{t}{2N} s(\{\zeta_i\}) \right] \approx 1$ in $A_p(t)$, yielding

$$A_p(t \ll N) \approx B_p + C_p \frac{t}{N}, \quad (3.24)$$

where the coefficients are

$$B_p = \sum_{n=2}^N \frac{(-1)^{n-1}}{n 2^n} \sum'_{\sum \zeta_i = p} r(\{\zeta_i\}), \quad C_p = \sum_{n=2}^N \frac{(-1)^n}{n 2^{n+1}} \sum'_{\sum \zeta_i = p} r(\{\zeta_i\}) s(\{\zeta_i\}). \quad (3.25)$$

The SFF expression becomes

$$\mathcal{K}_{t \ll N} = \frac{g_0^N}{D^{2N}} \exp \left[N \sum_{k=1}^L r_k \frac{J_1(2kt)}{kt} \cos(k\mu t) + N(B_0 + C_0 t) \right. \\ \left. + 2N \sum_{p=1}^{NL} (B_p + C_p t/N) \frac{\sin(\frac{\pi}{2} p t)}{\frac{\pi}{2} p t} \cos(p\mu t) \right]. \quad (3.26)$$

For physical consistency, we require

$$\lim_{N \rightarrow \infty} B_p = \text{finite}, \quad \lim_{N \rightarrow \infty} C_p/N = \text{finite}. \quad (3.27)$$

– Early Time: $0 < t \ll 1$

Neglecting C_p terms ($C_p t/N \ll B_p$), we obtain

$$\mathcal{K}_{t \ll 1} = \frac{g_0^N}{D^{2N}} \exp \left[N B_0 + N \sum_{k=1}^L r_k \frac{J_1(2kt)}{kt} \cos(k\mu t) + 2N \sum_{p=1}^{\infty} B_p \frac{\sin(\frac{\pi}{2} p t)}{\frac{\pi}{2} p t} \cos(p\mu t) \right]. \quad (3.28)$$

The normalization condition $\mathcal{K}(0) = 1$ imposes

$$2 \sum_{p=1}^{\infty} B_p = \log \left(1 + \sum_{k=1}^L r_k \right) - \sum_{k=1}^L r_k - B_0. \quad (3.29)$$

To second order in t

$$\frac{\log \mathcal{K}_{t \ll 1}}{N} = - \left[\left(\mu^2 + \frac{\pi^2}{12} \right) \sum_{p=1}^{\infty} p^2 B_p + \frac{\mu^2 + 1}{2} \sum_{k=1}^L k^2 r_k \right] t^2 + \mathcal{O}(t^4). \quad (3.30)$$

– Intermediate Time: $1 \ll t \ll N$

Dominant contribution comes from $A_0(t)$

$$\mathcal{K}_{1 \ll t \ll N} = \frac{g_0^N}{D^{2N}} \exp \left[N \sum_{k=1}^L r_k \frac{J_1(2kt)}{kt} \cos(k\mu t) + N B_0 + C_0 t \right]. \quad (3.31)$$

For $t \gg t_p \equiv (N/C_0)^{2/5}$, the exponential ramp dominates

$$\mathcal{K}_{t_p \ll t \ll N} = \frac{g_0^N}{D^{2N}} \exp [N B_0 + C_0 t]. \quad (3.32)$$

• Late Time: $t \gg N$

The step function vanishes, leaving

$$\mathcal{K}_{t \gg N} = \frac{g_0^N}{D^{2N}} \exp \left[N \sum_{k=1}^L r_k \frac{J_1(2kt)}{kt} \cos(k\mu t) \right]. \quad (3.33)$$

At infinite time, we have $\mathcal{K}_{t=\infty} = \frac{g_0^N}{D^{2N}}$, it is consistent with the coherent state approach result (Eq. (3.8)).

3.2.1 R -para-fermions with $z_R(x) = 1 + mx$

It is direct to find

$$|z_R|^2(t) = m^2 + 1 + 2m \cos(t(\varepsilon - \mu)), \quad (3.34)$$

then $g_0 = m^2 + 1, g_1 = 2m, D = m + 1$, so that we have

$$r_1 = \frac{2m}{m^2 + 1} \leq 1, \quad \xi_i = \pm 1. \quad (3.35)$$

Using the definition in Eq. (3.25), we have

$$\begin{aligned} B_0 &= \sum_{n=\text{even}, n \geq 2} \frac{(-1)^{n-1} r_1^n}{n 2^n} \binom{n}{\frac{n}{2}} = \log \left(\frac{1}{2} \left(\sqrt{1 - r_1^2} + 1 \right) \right), \\ B_1 &= \sum_{n=\text{odd}, n \geq 2} \frac{(-1)^{n-1} r_1^n}{n 2^n} \binom{n}{\frac{n-1}{2}} = \frac{2 - r_1^2 - 2\sqrt{1 - r_1^2}}{2r_1}. \end{aligned} \quad (3.36)$$

For $k > 1$, we have a universal relation

$$B_k = \frac{(-1)^{k-1}}{k} \left[\frac{\cos\left(\frac{\theta_1}{2}\right) - \sin\left(\frac{\theta_1}{2}\right)}{\cos\left(\frac{\theta_1}{2}\right) + \sin\left(\frac{\theta_1}{2}\right)} \right]^k, \quad r_1 = \cos \theta_1. \quad (3.37)$$

Then one can check the results are consistent with Eq. (3.29), moreover, they return back to the results in Appendix of [57] when $r_1 = 1$. For $t \ll 1$, we have

$$\frac{\log \mathcal{K}_{t \ll 1}}{N} = - \left[\frac{(\mu^2 + 1)m}{(m+1)^2} + \frac{(12 - \pi^2)m^2}{6(m+1)^2(m^2 + 1)} \right] t^2 + \mathcal{O}(t^4), \quad (3.38)$$

while the coherent state approach gives

$$\frac{\log \mathcal{K}_{t \ll 1}}{N} = - \frac{(\mu^2 + 1)m}{(m+1)^2} t^2 + \mathcal{O}(t^4). \quad (3.39)$$

The numerical simulation indicate the coherent state approach is exact for short time, the cluster approach with box approximation is not accurate. For C_0 , following the derivations in Appendix of [57], we have

$$C_0 = \sum_{n=\text{even}, n \geq 2}^N \frac{(-1)^n r_1^n}{n 2^{n+1}} \left(2^n - \frac{n!}{\left(\frac{n}{2}\right)! \left(\frac{n}{2}\right)!} \right). \quad (3.40)$$

So finally we obtain

$$C_0 = \begin{cases} -\frac{1}{4} \log(1 - r_1^2) + \frac{1}{2} \log \left(\frac{1}{2} \left(\sqrt{1 - r_1^2} + 1 \right) \right), & r_1 < 1, \\ \frac{1}{4} \left(\ln \frac{N}{8} + \gamma_E \right), & r_1 = 1. \end{cases}$$

One can see the dramatic transition from $m = 1$ to $m > 1$. We plot the theoretical and numerical result in Fig. 3. Notice that the Hilbert space has dimension D^N while the energy scale is proportional to N , so the energy gap between two neighbor levels are of order $\frac{N}{D^N}$, when it is small than the machine precise $\delta \approx 10^{-16}$ the simulation of GUE will break.

$$\frac{1}{D^N} = \delta \Rightarrow N = \log_D \delta. \quad (3.41)$$

For $D = 6$, $N = 20$. So that for numerical simulation, we can not take large N limit to compare with the results in the main text.

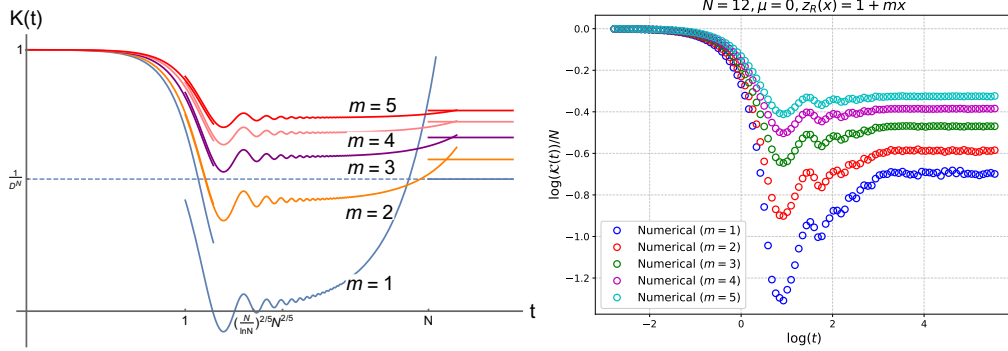


Figure 3. **Left:** Log-log plot of SFF using the cluster function approach for $z_R(x) = 1 + mx$ with $m = 1, 2, 3, 4, 5$ ($N = 400$). Time range $t \in [0.02, 8N]$. The $m = 1$ case (ordinary fermions) shows an exponential ramp with $C_0 \sim \mathcal{O}(\ln N)$, while $m > 1$ cases exhibit qualitatively different behavior with $C_0 \sim \mathcal{O}(1)$. **Right:** Numerical simulation for $N = 12$ with 20,000 samples ($t \in [2^{-4}, 2^8]$). While the small system size prevents observation of the exponential ramp, the plateau location agrees with the theoretical prediction $\mathcal{K}(t \rightarrow \infty) = (m^2 + 1)^N / (m + 1)^{2N}$.

3.2.2 R -para-fermions with $z_R(x) = 1 + mx + x^2$

Then we turn to deal with Example B, it is straightforward to obtain

$$|z_R|^2(t) = m^2 + 2 + 4m \cos(t(\varepsilon - \mu)) + 2 \cos(2t(\varepsilon - \mu)), \quad (3.42)$$

so that

$$r_1 = \frac{4m}{m^2 + 2}, r_2 = \frac{2}{m^2 + 2}, \zeta_i = \pm 1, \pm 2. \quad (3.43)$$

Unlike the former case, here one may have $r_1 > 1$. Define $Q(x) = r_1 x + r_1 x^{-1} + r_2 x^2 + r_2 x^{-2}$, we have

$$\sum_{\sum \zeta_i = p} r(\{\zeta_i\}) = Q(x)^n \Big|_{x^p}, \quad \sum_{\sum \zeta_i = 0} r(\{\zeta_i\}) s(\{\zeta_i\}) = 2 \sum_{l=1}^{\lfloor nL/2 \rfloor} Q(x)^n \Big|_{x^{2l}}. \quad (3.44)$$

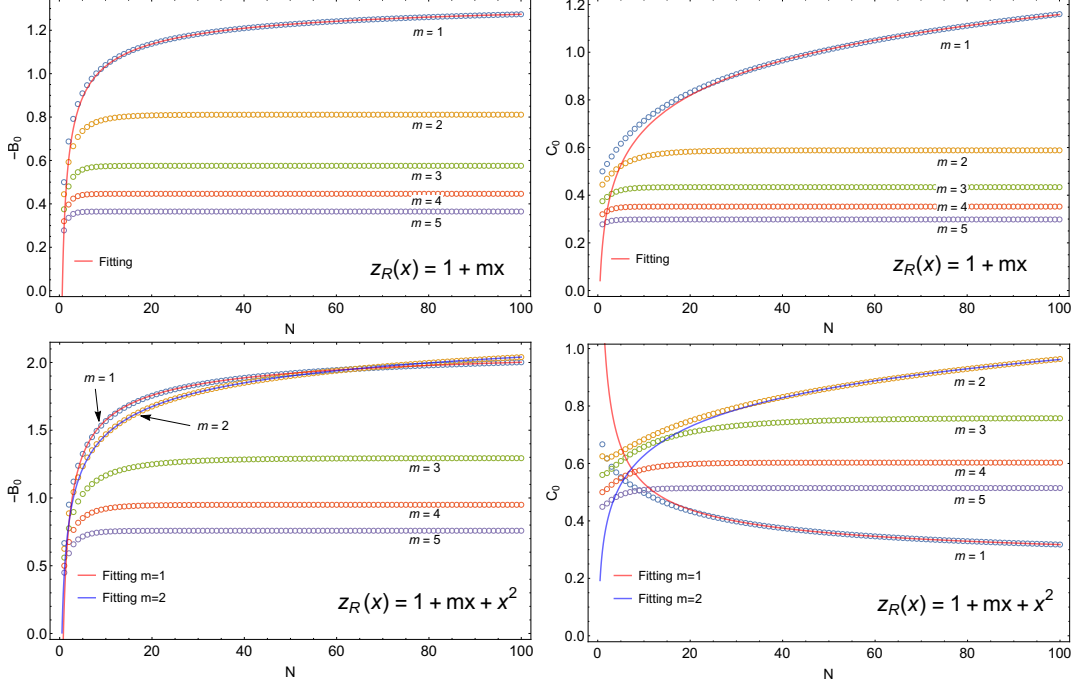


Figure 4. The plot of $-B_0, C_0$ with respect to N for $z_R(x) = 1 + mx$ and $z_R(x) = 1 + mx + x^2$. The fitting function for B_0 and convergent C_0 ($z_R(x) = 1 + mx + x^2$ with $m = 1$) takes the form $f(N) = a + \frac{b}{N^c}$. We choose $c = 1/4$ for $z_R(x) = 1 + mx + x^2$ with $m = 2$ and $c = 1/2$ for other cases. For the case $z_R(x) = 1 + mx, m = 1$ and $z_R(x) = 1 + mx + x^2, m = 2$, C_0 is divergent for large N , we fit it with $f(N) = a + b \log N$. Since we are concern to asymptotic behavior, we use the data $N \geq 40$ to fit.

We just need to evaluate scale of B_0, C_0 , It is hard to evaluate the B_0, C_0 analytically, so we may better to consider numerical method. But here $r_1 > 1$ for small m and $r_2 > 0$ so that the summation in the definition of B_p, C_p is not convergent numerically. We would better to use another expansion. Denote $|z_R|^2(t) = D^2(1 + F(\varepsilon, t))$, then we have

$$\begin{aligned}
\prod_{j=1}^n F(\varepsilon_j, t) &= \prod_{j=1}^n \left[\tilde{g}_0 - 1 + \sum_{k=1}^L \tilde{g}_k \cos(kt(\varepsilon_j - \mu)) \right] \\
&= \frac{1}{2^n} \sum_{\{\zeta\}=-L}^L \mathbf{g}_{\{\zeta\}} \exp\left(it \sum_{j=1}^n \zeta_j (\varepsilon_j - \mu) \right)
\end{aligned} \tag{3.45}$$

where we have defined

$$\mathbf{g}_0 = 2(\tilde{g}_0 - 1), \mathbf{g}_{k>0} = \tilde{g}_k. \tag{3.46}$$

After similar derivation, we have

$$\mathcal{K}(t) = \exp \left[N\mathbf{g}_0/2 + N \sum_{k=1}^L \mathbf{g}_k \frac{J_1(2kt)}{kt} \cos(k\mu t) + NA_0(t) + 2N \sum_{p=1}^{NL} A_p(t) \frac{\sin(\frac{\pi}{2}pt)}{\frac{\pi}{2}pt} \cos(p\mu t) \right] \quad (3.47)$$

where $A_p(t) = B_p + \frac{1}{N}C_p t$ as before, everything are the same, except each ζ_i can be 0. Since $\mathbf{g}_0 < 0$ and $|\mathbf{g}_0| < 2, 0 < \mathbf{g}_k < 1$, the numerical calculation converges fast. The definition of B_p, C_p is modified to

$$B_p = \sum_{n=2}^N \frac{(-1)^{n-1}}{n2^n} \sum_{\sum \zeta_i = p} \mathbf{g}(\{\zeta_i\}), \quad C_p = \sum_{n=2}^N \frac{(-1)^n}{n2^{n+1}} \sum_{\sum \zeta_i = p} \mathbf{g}(\{\zeta_i\})s(\{\zeta_i\}) \quad (3.48)$$

where each ζ_i take values $-L, -L+1, \dots, 0, 1, \dots, L-1, L$, so we remove l above the summation. After defining $Q(x) = \mathbf{g}_0 + \sum_{k=1}^L \mathbf{g}_k(x^k + x^{-k})$, we have

$$\sum_{\sum \zeta_i = 0} \mathbf{g}(\{\zeta_i\}) = Q(x)^n \Big|_{x^0}, \quad \sum_{\sum \zeta_i = 0} \mathbf{g}(\{\zeta_i\})s(\{\zeta_i\}) = 2 \sum_{l=1}^{\lfloor nL/2 \rfloor} Q(x)^n \Big|_{x^{2l}}. \quad (3.49)$$

One can evaluate B_0, C_0 analytically by using the expansion

$$Q(x)^n = \sum_{\{a\}} \binom{n}{a_0} \binom{n-a_0}{a_1} \binom{n-a_0-a_1}{a_2} \dots \binom{a_L}{a_L} \mathbf{g}_0^{a_0} \prod_{j=1}^L \mathbf{g}_j^{a_j} (x^j + x^{-j})^{a_j}. \quad (3.50)$$

But it will become over-complicated for $L > 1$. So we would better to calculate B_0, C_0 numerically.

Then the remaining thing is to determine the asymptotic behavior of B_0, C_0 for large N with numerical data. It is expected that B_0 is always convergent for large N , while for some cases, C_0 can be divergent as N goes to infinity. We assume the divergent behavior is $\log N$. Denote c_N as a numerical list of N (taking c_N to be B_0 or C_0). We determine if it is convergent by fitting data $N > N_* \gg 1$ with $a + b \log N$; if the error of fit for data $N < N_*$ is large, it means the fitting function is not appropriate and the list is convergent. For the convergent c_N which approaches its limit exponentially ($c_N \sim c_\infty + ae^{-bN}, b > 0$), we numerically take the approximation $c_\infty \approx c_{N_0}$ with a large but finite $N_0 \gg 1$. If c_N approaches its limit polynomially ($c_N \sim c_\infty + aN^{-b}, b > 0$), we first fit c_N with data for $N \geq N_*$, then take the limit $N \rightarrow \infty$ to obtain c_∞ , where a proper b is chosen so that the fitting function has a small error for the data near $N < N_*$. There is no need to determine b accurately, as the box approximation with the rough kernel $\mathbf{K}(\varepsilon_i, \varepsilon_j)$ is not accurate itself.

The numerical results for Example A, B are shown in Fig. 4. Here we will not calculate other B_p, C_p as they are not important for the ramp behavior. One can find B_0 is convergent for any case. As for C_0 , it becomes log-divergent only for the trivial R -PSYK₂ when $z_R(x) = (1+x)^m$, i.e., Example A with $m = 1$ and Example B with $m = 2$. This phenomenon leads

to a conjecture: A R -PSYK₂ has an exponential ramp with $C_0 \sim \ln N$ only when its $z_R(x)$ is trivial; otherwise, $C_0 \sim \mathcal{O}(1)$. For now, we can only check the conjecture numerically; its analytical proof requires a mathematical evaluation of the expression of C_0 .

4 Time Evolution

In this section, we examine the time evolution of $\psi_{i,a}^\pm$, which is essential for computing correlation functions. The exchange statistics between operators at different sites proves nontrivial, as each $\psi_{i,a}$ constitutes a global operator representable as a sum of MPO string operators acting on a spin chain. These operators $\psi_{i,a}^\pm$ act nontrivially on the first i spins.

Nevertheless, we can directly evaluate the time evolution. A more effective approach involves constructing the basis through local spin operators $x_{i,a}^\pm$ and $y_{i,a}^\pm$, where $x_{i,a}^\pm$ satisfies distinct commutation relations (see Eq. (S21) in the arXiv version of [13]). For general R , we have

$$\begin{aligned}\hat{\psi}_{ia}^- &= a \begin{array}{c} \text{---} \text{---} \text{---} \text{---} \text{---} \\ \diagup \quad \diagdown \quad \diagup \quad \diagdown \quad \diagup \\ \text{---} \text{---} \text{---} \text{---} \text{---} \\ 1 \quad 2 \quad 3 \quad \dots \quad i-1 \quad i \end{array}, \\ \hat{\psi}_{ia}^+ &= a \begin{array}{c} \text{---} \text{---} \text{---} \text{---} \text{---} \\ \diagdown \quad \diagup \quad \diagdown \quad \diagup \quad \diagdown \\ \text{---} \text{---} \text{---} \text{---} \text{---} \\ 1 \quad 2 \quad 3 \quad \dots \quad i-1 \quad i \end{array},\end{aligned}\quad (4.1)$$

where $\hat{y}_{ja}^\pm \equiv a \begin{array}{c} \text{---} \\ \diagup \\ \text{---} \\ j \end{array}$, and $\hat{T}_{j,ab}^\pm \equiv a \begin{array}{c} \text{---} \\ \diagup \quad \diagdown \\ \text{---} \\ j \end{array} b = \mp [\hat{y}_{j,a}^\pm, \hat{x}_{j,b}^\mp]$ are local spin operators acting on site j . Both $\hat{\psi}_{i,a}^\pm$ act non-trivially on sites $1, 2, \dots, i$ and act as identity on the rest of the chain. Explicitly, we have

$$\psi_{i,a}^\pm = T_{1,ab_1}^\pm \otimes T_{2,b_1b_2}^\pm \otimes \dots \otimes T_{i-1,b_{i-2}b_{i-1}}^\pm \otimes y_{i,b_{i-1}}^\pm = \left(\otimes_{k=1}^{i-1} T_k^\pm \right)_{ab} \otimes y_{i,b}^\pm \quad (4.2)$$

where the summation over b_i is omitted. For a local operator \hat{O}_k acting on the local Hilbert space of site k , we its time evolution is given by

$$\hat{O}_k(\beta + it) = e^{(-\beta+it)H} \hat{O}_k e^{(-\beta-it)H}, \quad (4.3)$$

with

$$H = \sum_{a=1}^m \sum_{k=1}^N \left(\frac{\hat{x}_{k,a}^+ \hat{y}_{k,a}^- + \hat{x}_{k,a}^- \hat{y}_{k,a}^+}{2} \varepsilon_k - \mu \hat{y}_{k,a}^+ \hat{y}_{k,a}^- \right) \equiv \sum_{k=1}^N H_k. \quad (4.4)$$

Since $[H_i, H_j] = 0, \forall i \neq j$, so that it is easy to obtain the time evolution of a local operator via

$$\hat{O}_k(\beta + it) = e^{(-\beta+it)H_k} \hat{O}_k e^{(-\beta-it)H_k}. \quad (4.5)$$

Note that all operators on the right-hand side of Eq. (4.2) are local, making their time evolution straightforward to compute since their matrix elements are known. With the time

evolution of the building blocks $\psi_{i,a}^\pm$ established, we can compute various correlation functions, including two-point functions and OTOCs (see [66] for the fermionic SYK₂ case). However, due to their complicated structure, performing the ensemble average may prove difficult. We omit explicit calculations here.

5 Conclusion

In this paper, we conduct a comprehensive investigation of the $q = 2$ para-Sachdev-Ye-Kitaev model (R -PSYK₂), analyzing both its thermodynamic properties and spectral form factor (SFF). Our results demonstrate that the coherent state approach provides an effective framework for studying finite-temperature behavior, while the cluster function approach with box approximation fails even at high temperatures. Moreover, through the coherent state formalism, we establish the self-averaging property of general R -PSYK₂ models in the large N limit.

Our analysis of the SFF reveals a notable transition in its ramp behavior. For the case $z_R(x) = 1 + mx$, we find analytically that $C_0 = \mathcal{O}(1)$ when $m > 1$, contrasting with the $C_0 = \mathcal{O}(\ln N)$ scaling observed in conventional SYK₂ models. Numerical studies of the case $z_R(x) = 1 + mx + x^2$ indicate that $C_0 = \mathcal{O}(1)$ for all parameter values except the trivial case $m = 2$. These results suggest that such transitions in C_0 may represent a universal characteristic of R -PSYK₂ systems, though other possible scaling behaviors remain to be explored.

The observed dramatic change in C_0 scaling at large N currently lacks a complete physical interpretation. Building on the gravitational connection established in [43], where the SYK SFF relates to double cone solutions, we note that our SFF computation involves only local quantities. This local nature allows for the replacement of $\psi_{i,a}^\pm$ with local spin operators $\hat{y}_{i,a}^\pm$ in the Hamiltonian, potentially enabling a path integral formulation—an interesting direction for future work. Mathematically, C_0 can be interpreted as a sum of weighted paths in Eq. (3.25). For $z_R(x) = 1 + mx$, the negative weight $r_1 < 0$ suggests convergence of C_0 as $N \rightarrow \infty$, though rigorous proof remains outstanding. Analytical treatment becomes increasingly difficult for higher-order $z_R(x)$, leading us to employ numerical methods based on Eq. (3.48). The slow (approximately logarithmic) growth of C_0 with N makes precise determination of scaling laws challenging, leaving open possibilities such as $C_0 \sim N^\alpha$ ($\alpha < 1$) or $C_0 \sim N^\alpha \ln N$.

While our focus has not been on correlation functions, their calculation follows directly from the methods developed in Section 4. Future studies could investigate how R -particle statistics influence two-point functions and out-of-time-ordered correlators (OTOCs). Another promising direction involves exploring matrix ensembles beyond the Gaussian unitary ensemble (GUE). Given the relative simplicity of R -PSYK₂, we are particularly interested in extending this work to R -PSYK _{$q > 2$} models to examine their thermodynamic properties, SFF behavior, and OTOC dynamics—all important topics for future research.

Acknowledgments

The graphical representations of the R -matrix and operators $\psi_{i,a}^{\pm}$ are adapted from the work of Zhiyuan Wang and Kaden R.A. Hazzard [13]. I am grateful to Yingyu Yang, Jianghui Yu, Yanyuan Li, and Professor Cheng Peng for their insightful discussions, as well as to Zhiyuan Wang, Chen-Te Ma, and Benjamin James Pethybridge for their kind comments and suggestions. T.L. acknowledges support from the National Natural Science Foundation of China (Grant No. 12175237).

A Cluster Function Approach

In this appendix, we present a detailed derivation of the cluster function approach for computing SFF. For any function $F(\varepsilon, t)$, we begin with the expectation value

$$\begin{aligned} \mathbb{E} \left(\prod_{j=1}^N [1 + F(\varepsilon_j, t)] \right) &= \frac{g_0^N}{D^{2N}} \int \prod_{i=1}^N d\varepsilon_i P_N(\varepsilon_1, \dots, \varepsilon_N) \prod_{j=1}^N [1 + F(\varepsilon_j, t)] \\ &= \frac{g_0^N}{D^{2N}} \left[1 + \sum_{n=1}^N \frac{1}{n!} \int R_n(\varepsilon_1, \dots, \varepsilon_n) \prod_{j=1}^n F(\varepsilon_j, t) d\varepsilon_j \right]. \end{aligned} \quad (\text{A.1})$$

Here, $R_n(\varepsilon_1, \dots, \varepsilon_n)$ represents the n -point single-particle energy level correlation function, defined as

$$R_n(\varepsilon_1, \dots, \varepsilon_n) = \frac{N!}{(N-n)!} \int d\varepsilon_{n+1} \dots d\varepsilon_N P_N(\varepsilon_1, \dots, \varepsilon_N). \quad (\text{A.2})$$

In the large- N limit, this correlation function is given by the determinant of the kernel $K(\varepsilon_i, \varepsilon_j)$, where

$$K(\varepsilon_i, \varepsilon_j) = \begin{cases} \frac{N}{2\pi} \sqrt{4 - \varepsilon_i^2} \Theta(2 - |\varepsilon_i|), & i = j, \\ \frac{N}{\pi} \frac{\sin[N(\varepsilon_i - \varepsilon_j)]}{N(\varepsilon_i - \varepsilon_j)}, & i \neq j. \end{cases} \quad (\text{A.3})$$

We then introduce the n -point cluster function

$$T_n(\varepsilon_1, \dots, \varepsilon_n) = \sum_{\mathcal{P}(n)} K(\varepsilon_1, \varepsilon_2) \cdots K(\varepsilon_{n-1}, \varepsilon_n) K(\varepsilon_n, \varepsilon_1), \quad (\text{A.4})$$

which leads to the compact expression

$$\mathcal{K}(t) = \exp \left[\sum_{n=1}^N \frac{(-1)^n}{n!} \bar{t}_n \right] \quad (\text{A.5})$$

with

$$\bar{\mathfrak{t}}_n = \int d\varepsilon_1 \dots d\varepsilon_n \mathfrak{T}_n(\varepsilon_1, \dots, \varepsilon_n) \prod_{i=1}^n F(\varepsilon_i, t). \quad (\text{A.6})$$

For both the partition function and SFF calculations considered in this work, the product of F functions can be expressed as sums

$$\prod_{j=1}^n F(\varepsilon_j, t) = \begin{cases} \sum_{\{\zeta\}} c_{\{\zeta\}} e^{it \sum_{j=1}^n \varepsilon_j \zeta_j} & (\text{SFF at infinite temperature}), \\ \sum_{\{\zeta\}} c'_{\{\zeta\}} e^{-\beta \sum_{j=1}^n \varepsilon_j \zeta_j} & (\text{Partition function}), \end{cases} \quad (\text{A.7})$$

where $\zeta_i \in \mathbb{Z}$. This formulation reduces our problem to evaluating two types of integrals

$$\begin{aligned} I_n(t\{\zeta_i\}) &\equiv \int d\varepsilon_1 \dots d\varepsilon_n \mathbf{K}(\varepsilon_1, \varepsilon_2) \dots \mathbf{K}(\varepsilon_n, \varepsilon_1) e^{it \sum_{i=1}^n \varepsilon_i \zeta_i}, \\ I_n^E(\beta\{\zeta_i\}) &\equiv \int d\varepsilon_1 \dots d\varepsilon_n \mathbf{K}(\varepsilon_1, \varepsilon_2) \dots \mathbf{K}(\varepsilon_n, \varepsilon_1) e^{-\beta \sum_{i=1}^n \varepsilon_i \zeta_i}. \end{aligned} \quad (\text{A.8})$$

While one might expect $I_n^E(\{\zeta_i\})$ to be simply related to $I_n(\{\zeta_i\})$ by analytic continuation $t \rightarrow i\beta$, this proves nontrivial in practice. To evaluate $I_n^E(\{\zeta_i\})$, we employ the box approximation (detailed in Eq. (S21) of [57]), yielding

$$I_1(\zeta_1 t) = N \frac{J_1(2|\zeta_1|t)}{|\zeta_1|t}, \quad (\text{A.9})$$

$$I_{n \geq 2}(t\{\zeta_i\}) = N \frac{\sin \left[\frac{\pi}{2} \left(t \sum_{j=1}^n \zeta_j \right) \right]}{\frac{\pi}{2} \left(t \sum_{j=1}^n \zeta_j \right)} \left[1 - \frac{t}{2N} s(\{\zeta_i\}) \right] \Theta \left[1 - \frac{t}{2N} s(\{\zeta_i\}) \right], \quad (\text{A.10})$$

where

$$s(\{\zeta_i\}) = \max \left\{ 0, \sum_{i=1}^j \zeta_i \right\}_{j=1}^{n-1} - \min \left\{ 0, \sum_{i=1}^j \zeta_i \right\}_{j=1}^{n-1}. \quad (\text{A.11})$$

The presence of the Heaviside theta function $\Theta(x)$, defined only for real x , prevents a naive analytic continuation to obtain $I_n^E(\{\zeta_i\})$. Following [67], where the box approximation was justified for infinite temperature, we extend this approach to the high-temperature limit ($\beta \ll 1$). By neglecting the term $\left[1 - \frac{t}{2N} s(\{\zeta_i\}) \right] \Theta \left[1 - \frac{t}{2N} s(\{\zeta_i\}) \right]$ in Eq. (A.9) and substituting $t \rightarrow i\beta$, we obtain

$$I_1^E(\beta\zeta) = N {}_0F_1(2; \beta^2 \zeta^2), \quad (\text{A.12})$$

$$I_{n \geq 2}^E(\beta\{\zeta\}) = N \frac{\sinh \left(\frac{\pi\beta}{2} \sum_{i=1}^n \zeta_i \right)}{\frac{\pi\beta}{2} \sum_{i=1}^n \zeta_i}. \quad (\text{A.13})$$

B Coherent State Approach

For any quantity $G = \prod_{i=1}^N \mathcal{G}(\varepsilon_i)$, we use the exact expression

$$P(\varepsilon_1, \dots, \varepsilon_N) = \frac{(N/2)^{N/2}}{N!} \sum_{i,j} \varepsilon_{\{i\}}^{\{j\}} \prod_{k=1}^N e^{-N\varepsilon_k^2/2} \mathbf{H}_{i_k-1} \left(\sqrt{\frac{N}{2}} \varepsilon_k \right) \mathbf{H}_{j_k-1} \left(\sqrt{\frac{N}{2}} \varepsilon_k \right), \quad (\text{B.1})$$

where $\mathbf{H}_k(x) = \frac{1}{\sqrt{2^k k! \sqrt{\pi}}} H_k(x)$ are the normalized Hermite polynomials. We then find

$$\begin{aligned} \langle G \rangle &= \frac{(N/2)^{N/2}}{N!} \sum_{i,j} \varepsilon_{\{i\}}^{\{j\}} \prod_{k=1}^N \int d\varepsilon_k e^{-N\varepsilon_k^2/2} \mathbf{H}_{i_k-1} \left(\sqrt{\frac{N}{2}} \varepsilon_k \right) \mathbf{H}_{j_k-1} \left(\sqrt{\frac{N}{2}} \varepsilon_k \right) \prod_{i=1}^N \mathcal{G}(\varepsilon_i) \\ &= \frac{1}{N!} \sum_{i,j} \varepsilon_{\{i\}}^{\{j\}} \prod_{k=1}^N \int dx e^{-x^2} \mathbf{H}_{i_k-1}(x) \mathbf{H}_{j_k-1}(x) \prod_{i=1}^N \mathcal{G} \left(x \sqrt{\frac{2}{N}} \right) \\ &= \det \mathbf{M}, \end{aligned} \quad (\text{B.2})$$

where

$$\begin{aligned} \mathbf{M}_{ij} &= \int dx e^{-x^2} \mathbf{H}_{i-1}(x) \mathbf{H}_{j-1}(x) g \left(x \sqrt{\frac{2}{N}} \right) \\ &= \langle i-1 | g \left(\hat{x} \sqrt{\frac{2}{N}} \right) | j-1 \rangle. \end{aligned} \quad (\text{B.3})$$

Noting that $e^{-x^2/2} \mathbf{H}_k(x)$ is the k -th wavefunction of a quantum harmonic oscillator with $m = \omega = 1$, we can treat x as an operator. We evaluate the large N limit as

$$\frac{1}{N} \log \langle G \rangle = \frac{1}{N} \log \det \mathbf{M} \approx \frac{1}{N} \sum_{i=1}^N \log \lambda_i, \quad (\text{B.4})$$

where λ_i are the eigenvalues of the operator $g \left(\hat{x} \sqrt{\frac{2}{N}} \right)$. Note that \mathbf{M} is an N -dimensional matrix obtained by truncating the infinite-dimensional matrix $g \left(\hat{x} \sqrt{\frac{2}{N}} \right)$, so its eigenvalues are not exactly the same. However, we expect the approximation in Eq. (B.3) to hold for large N . Using the relation $\hat{x} = \frac{1}{\sqrt{2}}(a + a^\dagger)$, where a and a^\dagger are the harmonic oscillator ladder operators, we employ coherent states $|\alpha\rangle$ (eigenstates of a) as our basis

$$\langle \alpha | \alpha' \rangle = \delta^2(\alpha - \alpha'), \quad \forall \alpha, \alpha' \in \mathbb{C}, \quad (\text{B.5})$$

$$\mathbb{I} = \int \frac{d^2\alpha}{\pi} |\alpha\rangle \langle \alpha|. \quad (\text{B.6})$$

The trace in Eq. (B.4) can be interpreted as a truncated trace in the harmonic oscillator Hilbert space

$$\text{tr}_N(\bullet) \equiv \text{tr}(\mathbb{I}_N \bullet) = \sum_{k=0}^{N-1} \langle k | \bullet | k \rangle \Rightarrow \frac{1}{N} \log \langle G \rangle \approx \frac{1}{N} \text{tr}_N \log \left[\mathcal{G} \left(\hat{x} \sqrt{\frac{2}{N}} \right) \right], \quad (\text{B.7})$$

where $\mathbb{I}_N = \sum_{i=0}^{N-1} |i\rangle\langle i|$ is the projector onto the first N states. For the coherent state basis, we restrict the trace to states with $|\alpha| \leq R$ and take the following replacements

$$N = \text{tr}_R \mathbb{I} = R^2, \quad (\text{B.8})$$

$$\text{tr}_N A \rightarrow \text{tr}_R(A) = \int_{|\alpha| < R} \frac{d^2\alpha}{\pi} A(\alpha, \alpha^*), \quad (\text{B.9})$$

$$\hat{x} \sqrt{\frac{2}{N}} \rightarrow \frac{1}{R}(a + a^\dagger). \quad (\text{B.10})$$

To quantify the difference between the two trace methods, we project $|n\rangle$ onto the coherent

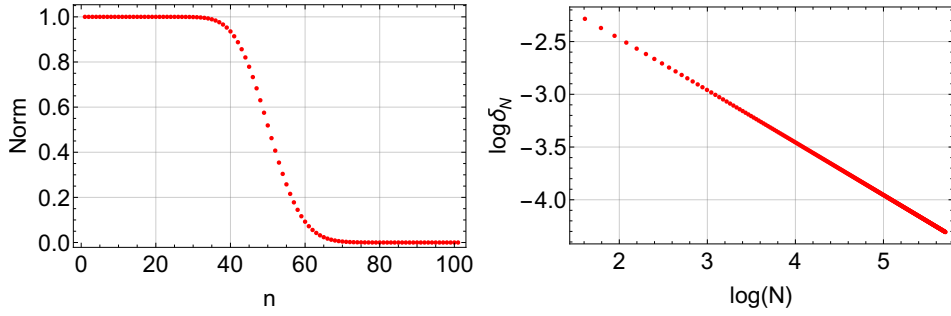


Figure 5. Left: Norm from Eq. (B.11) with $N = 50$. Right: Log-log plot of the error in Eq. (B.12).

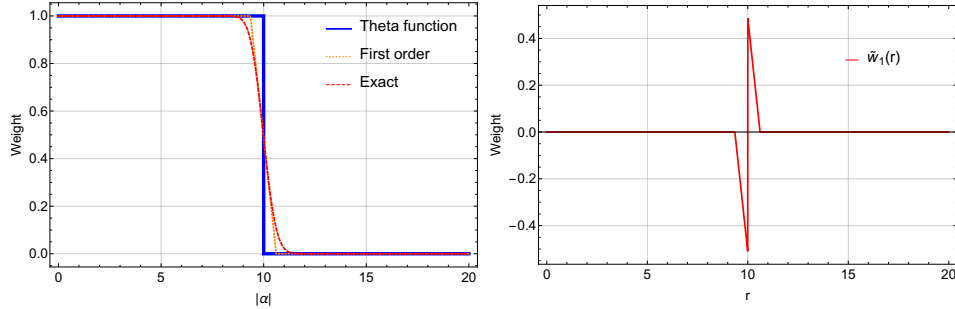


Figure 6. Leading-order and first-order approximations of the weight function.

state basis and compute the norm w_n

$$\begin{aligned} w_n &= \int_{|\alpha| \leq R} \frac{d^2\alpha}{\pi} |\langle n|\alpha\rangle|^2 = \int_{|\alpha| \leq R} \frac{d^2\alpha}{\pi} e^{-|\alpha|^2} \frac{|\alpha|^{2n}}{n!} \\ &= R^2 \int_0^1 \int_0^{2\pi} \frac{u du d\theta}{\pi} e^{-u^2 R^2} \frac{u^{2n} R^{2n}}{n!} = 1 - \frac{\Gamma(n+1, N)}{\Gamma(n+1)}. \end{aligned} \quad (\text{B.11})$$

The error between the exact and approximate traces is measured by

$$\delta_N = \frac{1}{N} \sum_{n=0}^{\infty} (w_n - w_n^{\text{exact}})^2 \sim \frac{a}{N^b}, \quad (\text{B.12})$$

$$a \approx 0.229955, \quad b \approx 0.497012. \quad (\text{B.13})$$

The vanishing of δ_N as $N \rightarrow \infty$ confirms the equivalence of the two traces in this limit. For $R \gg 1$, we approximate the trace as

$$\begin{aligned} \frac{1}{N} \log \langle G \rangle &\approx \frac{1}{R^2} \text{tr}_R \log \left[g \left(\frac{a + a^\dagger}{R} \right) \right] \\ &\approx \int_0^1 \int_0^{2\pi} \frac{u \, du \, d\theta}{\pi} \log [g(2u \cos \theta)], \end{aligned} \quad (\text{B.14})$$

where we used polar coordinates $\alpha = R u e^{i\theta}$. For operators of the form $A = e^{\lambda(a+a^\dagger)}$, which satisfy $A|\alpha\rangle = e^{\lambda(\alpha^* + \alpha - 1/2)}|\alpha\rangle$, we have:

$$\text{tr}_N(A) = \sum_{n=0}^{N-1} \int \frac{d^2\alpha}{\pi} e^{-|\alpha|^2} \frac{|\alpha|^{2n}}{n!} A(\alpha, \alpha^*). \quad (\text{B.15})$$

The weight function approximation can be improved by expanding near $r = R = \sqrt{N}$

$$w(r) = \begin{cases} 1, & r < r_a, \\ w_p(r), & r_a \leq r \leq r_b, \\ 0, & r > r_b, \end{cases} \quad (\text{B.16})$$

where $w_p(r) = \sum_{j=0}^p c_j (r - R)^j$. The first-order approximation gives

$$\begin{aligned} w_1(r) &= \frac{\Gamma(N, N)}{\Gamma(N)} - \frac{2e^{-N} N^{N+\frac{1}{2}} (r - \sqrt{N})}{\Gamma(N+1)}, \\ r_a &= \sqrt{N} - \frac{N^{-N-\frac{1}{2}} e^N (\Gamma(N)^2 - \Gamma(N)\Gamma(N, N))}{2\Gamma(N)}, \\ r_b &= \sqrt{N} + \frac{N^{-N-\frac{1}{2}} e^N \Gamma(N+1)\Gamma(N, N)}{2\Gamma(N)}. \end{aligned} \quad (\text{B.17})$$

In the large N limit, we find

$$\lim_{N \rightarrow \infty} \frac{\Gamma(N, N)}{\Gamma(N)} = \frac{1}{2}, \quad (\text{B.18})$$

$$\lim_{N \rightarrow \infty} \frac{\sqrt{N} - r_a}{r_b - \sqrt{N}} = 1, \quad (\text{B.19})$$

which suggests the first-order approximation

$$w(r) \approx \Theta(\sqrt{N} - r) + \tilde{w}_1(r). \quad (\text{B.20})$$

The leading-order and first-order approximations are compared in Fig. 6.

References

- [1] J. M. Leinaas and J. Myrheim, *On the theory of identical particles*, *Nuovo Cimento B Serie* **37** (Jan., 1977) 1–23.
- [2] F. Wilczek, *Quantum mechanics of fractional-spin particles*, *Phys. Rev. Lett.* **49** (Oct, 1982) 957–959.
- [3] F. Wilczek, *Fractional Statistics and Anyon Superconductivity*. World Scientific, Singapore, 1990.
- [4] C. Nayak, S. H. Simon, A. Stern, M. Freedman, and S. Das Sarma, *Non-abelian anyons and topological quantum computation*, *Reviews of Modern Physics* **80** (Sept., 2008) 1083–1159.
- [5] A. Stern, *Anyons and the quantum Hall effect—A pedagogical review*, *Annals of Physics* **323** (Jan., 2008) 204–249, [[arXiv:0711.4697](https://arxiv.org/abs/0711.4697)].
- [6] H. S. Green, *A generalized method of field quantization*, *Phys. Rev.* **90** (Apr, 1953) 270–273.
- [7] H. Araki, *On the connection of spin and commutation relations between different fields*, *Journal of Mathematical Physics* **2** (05, 1961) 267–270, [https://pubs.aip.org/aip/jmp/article-pdf/2/3/267/19046477/267_1_online.pdf].
- [8] O. W. Greenberg and A. M. L. Messiah, *Selection rules for parafields and the absence of para particles in nature*, *Phys. Rev.* **138** (Jun, 1965) B1155–B1167.
- [9] P. Landshoff and H. P. Stapp, *Parastatistics and a unified theory of identical particles*, *Annals of Physics* **45** (1967), no. 1 72–92.
- [10] K. Drühl, R. Haag, and J. E. Roberts, *On parastatistics*, *Communications in Mathematical Physics* **18** (sep, 1970) 204–226.
- [11] R. H. Stolt and J. R. Taylor, *Correspondence between the first- and second-quantized theories of paraparticles*, *Nuclear Physics B* **19** (1970), no. 1 1–19.
- [12] D. J. Baker, H. Halvorson, and N. Swanson, *The conventionality of parastatistics*, *British Journal for the Philosophy of Science* **66** (Dec., 2015) 929–976.
- [13] Z. Wang and K. R. A. Hazzard, *Particle exchange statistics beyond fermions and bosons*, *Nature* **637** (Jan., 2025) 314–318.
- [14] Z. Wang, *Parastatistics and a secret communication challenge*, 2025.
- [15] M. Mekonnen, T. D. Galley, and M. P. Mueller, *Invariance under quantum permutations rules out parastatistics*, 2025.
- [16] V. Turaev, *The yang-baxter equation and invariants of links*, *Inventiones mathematicae* **92** (1988) 527–553.
- [17] S. Majid, *Examples of braided groups and braided matrices*, *Journal of Mathematical Physics* **32** (12, 1991) 3246–3253, [https://pubs.aip.org/aip/jmp/article-pdf/32/12/3246/19306681/3246_1_online.pdf].
- [18] P. Etingof, T. Schedler, and A. Soloviev, *Set-theoretical solutions to the quantum yang-baxter equation*, 1998.
- [19] A. Kitaev, “Hidden correlations in the Hawking radiation and thermal noise.” Talk at the Fundamental Physics Prize Symposium. November 10, 2014.

- [20] A. Kitaev, “A simple model of quantum holography.” Talks at KITP.
- [21] J. Polchinski and V. Rosenhaus, *The spectrum in the sachdev-ye-kitaev model*, *Journal of High Energy Physics* **2016** (Apr., 2016) 1–25.
- [22] J. Maldacena and D. Stanford, *Remarks on the sachdev-ye-kitaev model*, *Physical Review D* **94** (Nov., 2016).
- [23] A. Jevicki, K. Suzuki, and J. Yoon, *Bi-Local Holography in the SYK Model*, *JHEP* **07** (2016) 007, [[arXiv:1603.06246](#)].
- [24] A. Jevicki and K. Suzuki, *Bi-local holography in the syk model: Perturbations*, 2016.
- [25] A. Kitaev and S. J. Suh, *The soft mode in the Sachdev-Ye-Kitaev model and its gravity dual*, *JHEP* **05** (2018) 183, [[arXiv:1711.08467](#)].
- [26] E. Witten, *An SYK-Like Model Without Disorder*, *J. Phys. A* **52** (2019), no. 47 474002, [[arXiv:1610.09758](#)].
- [27] W. Fu, D. Gaiotto, J. Maldacena, and S. Sachdev, *Supersymmetric Sachdev-Ye-Kitaev models*, *Phys. Rev. D* **95** (2017), no. 2 026009, [[arXiv:1610.08917](#)]. [Addendum: *Phys.Rev.D* 95, 069904 (2017)].
- [28] I. R. Klebanov and G. Tarnopolsky, *Uncolored random tensors, melon diagrams, and the Sachdev-Ye-Kitaev models*, *Phys. Rev. D* **95** (2017), no. 4 046004, [[arXiv:1611.08915](#)].
- [29] D. J. Gross and V. Rosenhaus, *A Generalization of Sachdev-Ye-Kitaev*, *JHEP* **02** (2017) 093, [[arXiv:1610.01569](#)].
- [30] M. Berkooz, P. Narayan, M. Rozali, and J. Simón, *Higher Dimensional Generalizations of the SYK Model*, *JHEP* **01** (2017) 138, [[arXiv:1610.02422](#)].
- [31] J. Murugan, D. Stanford, and E. Witten, *More on Supersymmetric and 2d Analogs of the SYK Model*, *JHEP* **08** (2017) 146, [[arXiv:1706.05362](#)].
- [32] C. Peng, *Vector models and generalized SYK models*, *JHEP* **05** (2017) 129, [[arXiv:1704.04223](#)].
- [33] C. Peng, M. Spradlin, and A. Volovich, *A Supersymmetric SYK-like Tensor Model*, *JHEP* **05** (2017) 062, [[arXiv:1612.03851](#)].
- [34] Y. Gu, A. Kitaev, S. Sachdev, and G. Tarnopolsky, *Notes on the complex Sachdev-Ye-Kitaev model*, *JHEP* **02** (2020) 157, [[arXiv:1910.14099](#)].
- [35] M. Berkooz, M. Isachenkov, V. Narovlansky, and G. Torrents, *Towards a full solution of the large N double-scaled SYK model*, *JHEP* **03** (2019) 079, [[arXiv:1811.02584](#)].
- [36] J. Maldacena, S. H. Shenker, and D. Stanford, *A bound on chaos*, *Journal of High Energy Physics* **2016** (Aug., 2016).
- [37] D. E. Parker, X. Cao, A. Avdoshkin, T. Scaffidi, and E. Altman, *A Universal Operator Growth Hypothesis*, *Phys. Rev. X* **9** (2019), no. 4 041017, [[arXiv:1812.08657](#)].
- [38] Y. Gu, X.-L. Qi, and D. Stanford, *Local criticality, diffusion and chaos in generalized Sachdev-Ye-Kitaev models*, *JHEP* **05** (2017) 125, [[arXiv:1609.07832](#)].
- [39] D. A. Roberts, D. Stanford, and A. Streicher, *Operator growth in the SYK model*, *JHEP* **06** (2018) 122, [[arXiv:1802.02633](#)].
- [40] J. Maldacena and X.-L. Qi, *Eternal traversable wormhole*, [arXiv:1804.00491](#).

- [41] J. Maldacena, D. Stanford, and Z. Yang, *Diving into traversable wormholes*, *Fortsch. Phys.* **65** (2017), no. 5 1700034, [[arXiv:1704.05333](#)].
- [42] P. Nayak, A. Shukla, R. M. Soni, S. P. Trivedi, and V. Vishal, *On the Dynamics of Near-Extremal Black Holes*, *JHEP* **09** (2018) 048, [[arXiv:1802.09547](#)].
- [43] P. Saad, S. H. Shenker, and D. Stanford, *A semiclassical ramp in SYK and in gravity*, [arXiv:1806.06840](#).
- [44] G. Sárosi, *AdS₂ holography and the SYK model*, *PoS Modave2017* (2018) 001, [[arXiv:1711.08482](#)].
- [45] D. J. Gross and V. Rosenhaus, *The Bulk Dual of SYK: Cubic Couplings*, *JHEP* **05** (2017) 092, [[arXiv:1702.08016](#)].
- [46] R. A. Davison, W. Fu, A. Georges, Y. Gu, K. Jensen, and S. Sachdev, *Thermoelectric transport in disordered metals without quasiparticles: The Sachdev-Ye-Kitaev models and holography*, *Phys. Rev. B* **95** (2017), no. 15 155131, [[arXiv:1612.00849](#)].
- [47] S. A. Hartnoll, A. Lucas, and S. Sachdev, *Holographic quantum matter*, [arXiv:1612.07324](#).
- [48] X.-Y. Song, C.-M. Jian, and L. Balents, *Strongly Correlated Metal Built from Sachdev-Ye-Kitaev Models*, *Phys. Rev. Lett.* **119** (2017), no. 21 216601, [[arXiv:1705.00117](#)].
- [49] D. Chowdhury, A. Georges, O. Parcollet, and S. Sachdev, *Sachdev-Ye-Kitaev models and beyond: Window into non-Fermi liquids*, *Rev. Mod. Phys.* **94** (2022), no. 3 035004, [[arXiv:2109.05037](#)].
- [50] H. W. Lin, *The bulk Hilbert space of double scaled SYK*, *JHEP* **11** (2022) 060, [[arXiv:2208.07032](#)].
- [51] V. Narovlansky and H. Verlinde, *Double-scaled SYK and de Sitter Holography*, [arXiv:2310.16994](#).
- [52] L. Susskind, *De Sitter Space, Double-Scaled SYK, and the Separation of Scales in the Semiclassical Limit*, [arXiv:2209.09999](#).
- [53] C. Peng, *$\mathcal{N} = (0, 2)$ SYK, Chaos and Higher-Spins*, *JHEP* **12** (2018) 065, [[arXiv:1805.09325](#)].
- [54] P. Gao, *Commuting SYK: a pseudo-holographic model*, *JHEP* **01** (2024) 149, [[arXiv:2306.14988](#)].
- [55] P. Gao, H. Lin, and C. Peng, *D-commuting SYK model: building quantum chaos from integrable blocks*, [arXiv:2411.12806](#).
- [56] P. H. C. Lau, C.-T. Ma, J. Murugan, and M. Tezuka, *Randomness and chaos in qubit models*, *Physics Letters B* **795** (Aug., 2019) 230–235.
- [57] Y. Liao, A. Vikram, and V. Galitski, *Many-body level statistics of single-particle quantum chaos*, *Physical Review Letters* **125** (Dec., 2020).
- [58] M. Winer, S.-K. Jian, and B. Swingle, *Exponential ramp in the quadratic sachdev-ye-kitaev model*, *Physical Review Letters* **125** (Dec., 2020).
- [59] P. H. Chris Lau, C.-T. Ma, J. Murugan, and M. Tezuka, *Correlated disorder in the syk₂ model*, *Journal of Physics A: Mathematical and Theoretical* **54** (Feb., 2021) 095401.

- [60] A. Legramandi, S. Bandyopadhyay, and P. Hauke, *Many-body spectral transitions through the lens of variable-range syk2 model*, 2024.
- [61] P. Lydzba, Y. Zhang, M. Rigol, and L. Vidmar, *Single-particle eigenstate thermalization in quantum-chaotic quadratic hamiltonians*, *Physical Review B* **104** (Dec., 2021).
- [62] C. Liu, X. Chen, and L. Balents, *Quantum entanglement of the sachdev-ye-kitaev models*, *Physical Review B* **97** (June, 2018).
- [63] P. Lydzba, M. Rigol, and L. Vidmar, *Entanglement in many-body eigenstates of quantum-chaotic quadratic hamiltonians*, *Physical Review B* **103** (Mar., 2021).
- [64] A. Legramandi and N. Talwar, *The moments of the spectral form factor in syk*, 2024.
- [65] B. J. Pethybridge, *Notes on complex $q = 2$ syk*, 2024.
- [66] A. M. García-García, C. Liu, L. Sá, J. J. M. Verbaarschot, and J. ping Zheng, *Anatomy of information scrambling and decoherence in the integrable sachdev-ye-kitaev model*, 2025.
- [67] J. Cotler, N. Hunter-Jones, J. Liu, and B. Yoshida, *Chaos, complexity, and random matrices*, *Journal of High Energy Physics* **2017** (Nov., 2017).